QCD Phenomenology – Parton Distributions

Robert Thorne

January 13, 2014

University College London

Hadrons are bound together by the strong force, described QCD.

The strong coupling constant $\alpha_S(\mu^2)$ runs with the energy scale μ^2 of a process, decreasing as μ^2 increases (**asymptotic freedom**).

$$\alpha_s(\mu^2) \approx \frac{4\pi}{(11 - 2/3N_f)\ln(\mu^2/\Lambda^2_{QCD})}$$

$\alpha_s(\mu^2)$ is very large if $\mu^2 \sim \Lambda^2_{\rm QCD}$ ($\sim 0.3{\rm GeV}$), the scale of nonperturbative physics, but $\alpha_s(\mu^2) \ll 1$ if $\mu^2 \gg \Lambda^2_{\rm QCD}$, and perturbation theory can be used.

Because of the strong force it is difficult to perform analytic calculations of scattering processes involving hadronic particles from first principles. However, the weakening of $\alpha_S(\mu^2)$ at higher scales $\rightarrow$ the **Factorization Theorem** – separates processes into nonperturbative **parton distributions** which describe the composition of the proton and can be determined from experiment, and perturbative **coefficient functions** associated with higher scales which are calculated as a power-series in $\alpha_S(\mu^2)$.

Hadron scattering with an electron factorizes.

Q^2 – Scale of scattering

$x = \frac{Q^2}{2P \cdot q}$ – Momentum fraction of parton.

In proton rest frame $P \cdot q = M_P \nu$ where ν =energy transfer.

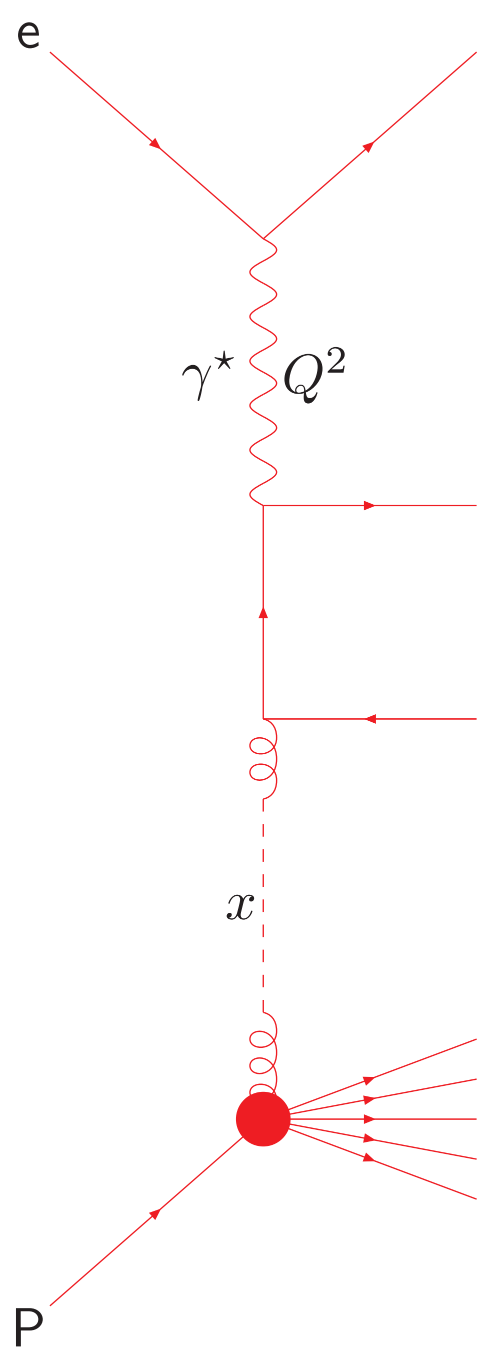

perturbative
calculable
coefficient function
$C_i^P(x, \alpha_s(Q^2))$

nonperturbative
incalculable
parton distribution
$f_i(x, Q^2, \alpha_s(Q^2))$

The cross-section for this process can be written in the factorized form

$$\sigma(ep \to eX) = \sum_i C_i^P(x, \alpha_s(Q^2)) \otimes \tilde{f}_i(x, Q^2, \alpha_s(Q^2))$$

$$\text{where} \qquad \left(a(x) \otimes b(x) = \int_x^1 a(z) b(x/z)\, dz\right)$$

$f_i(x, Q^2, \alpha_s(Q^2))$ represents the probability to find a parton of type i carrying a fraction x of the momentum of the hadron and $\tilde{f}_i(x, Q^2) = x f_i(x, Q^2)$.

Corrections to above formula of size $\Lambda^2_{\rm QCD}/Q^2$.

The partons are intrinsically nonperturbative. However, once Q^2 is large enough they do evolve with Q^2 in a perturbative manner.

$$\frac{d\tilde{f}_i(x, Q^2, \alpha_s(Q^2))}{d \ln Q^2} = \sum_j P_{ij}(x, \alpha_s(Q^2)) \otimes \tilde{f}_j(x, Q^2, \alpha_s(Q^2))$$

where the splitting functions $P_{ij}(x, Q^2, \alpha_s(Q^2))$ describing how a parton splits into more partons are calculable order by order in perturbation theory.

Partons parametrised at one low scale Q_0^2, evolved to higher Q^2.

The coefficient functions $C_i^P(x, \alpha_s(Q^2))$ are process dependent (new physics) but are calculable as a power-series in $\alpha_s(Q^2)$.

$$C_i^P(x, \alpha_s(Q^2)) = \sum_k C_i^{P,k}(x)\alpha_s^k(Q^2).$$

Since the parton distributions $f_i(x, Q^2, \alpha_s(Q^2))$ are process-independent, i.e. **universal**, once they have been measured at one experiment, one can predict many other scattering processes.

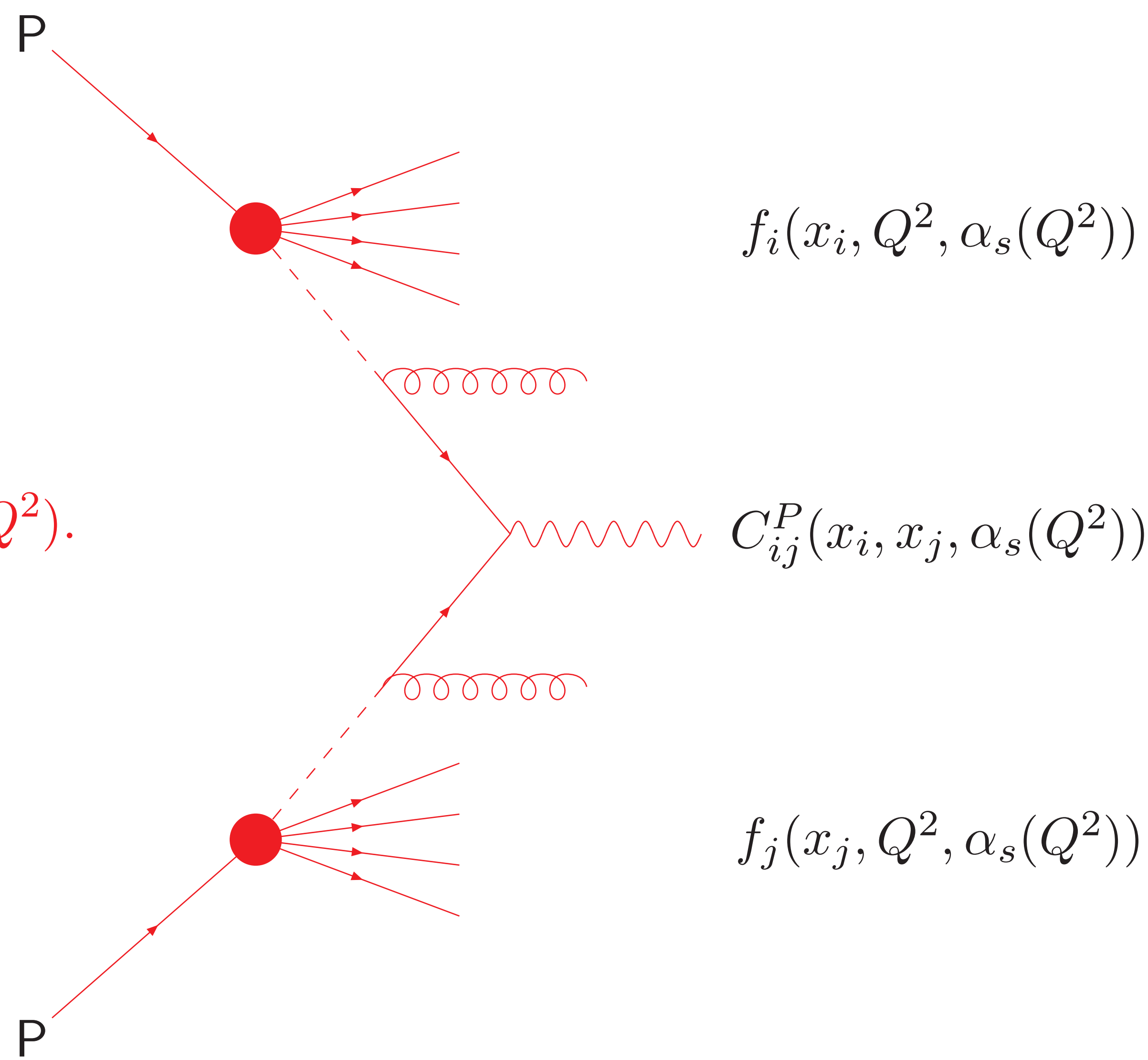

Global fits to determine parton distributions use all available data - largely $ep \to eX$ (Structure Functions), and the most up-to-date QCD calculations to best determine **parton distributions** and their consequences. Currently use NLO–in–$\alpha_s(Q^2)$, i.e.

$$\begin{aligned} C_i^P(x,\alpha_s(Q^2)) &= C_i^{P,0}(x) + \alpha_S(Q^2)C_i^{P,0}(x). \\ P_{ij}(x,\alpha_s(Q^2)) &= \alpha_S(Q^2)P_{ij}^0(x) + \alpha_S^2(Q^2)P_{ij}(x). \end{aligned}$$

NNLO coefficient functions are known for some processes, e.g. structure functions, and NNLO splitting functions have very recently been completed. Full NNLO fits just about possible with but some (very good) approximations.

Perturbation theory valid if $\alpha_s(Q^2) < 0.3$. Since running coupling constant $\alpha_s(Q^2)$

$$\alpha_s(Q^2) \approx \frac{4\pi}{(11 - 2/3N_f)\ln(Q^2/\Lambda^2_{QCD})}$$

where Λ_{QCD} is the scale of hadronic physics, i.e $\sim 150\mathrm{MeV}$, can use perturbation theory if $Q^2 > 2\mathrm{GeV}^2$. This cut should also remove influence of higher twists.

General procedure.

Start parton evolution at low scale $Q_0^2 \sim 1\mathrm{GeV}^2$, and fit data for scales above $2\mathrm{GeV}^2$. In principle 11 different parton distributions to consider

$$u, \bar{u}, \quad d, \bar{d}, \quad s, \bar{s}, \quad c, \bar{c}, \quad b, \bar{b}, \quad g$$

$m_c, m_b \gg \Lambda_{\mathrm{QCD}}$ so heavy parton distributions determined perturbatively. Assume $s = \bar{s}$. Leaves 6 independent combinations. Normally use $s(Q_0^2) = \kappa 1/2(\bar{u}(Q_0^2) + \bar{d}(Q_0^2))$, where in practice $\kappa \approx 0.4$. Then use

$$u_V = u - \bar{u}, \quad d_V = d - \bar{d}, \quad \mathrm{sea} = 2 * (\bar{u} + \bar{d} + \bar{s}), \quad \bar{d} - \bar{u}, \quad g,$$

Input partons parametrised as, e.g.

$$xf(x, Q_0^2) = (1-x)^{\eta}(1 + \epsilon x^{0.5} + \gamma x)x^{\delta}.$$

For non-singlet combinations, valence quarks, $\bar{d} - \bar{u}$, δ expected to be ~ 0.5. For singlet combinations, sea and gluon, δ expected to be ~ 0.

Also define the singlet quark distribution

$$\Sigma = u_V + d_V + \mathrm{sea} + (c + \bar{c}) + (b + \bar{b})$$

Assuming isospin symmetry $p \rightarrow n$ leads to

$$d(x) \rightarrow u(x) \qquad u(x) \rightarrow d(x).$$

Various sum rules constraining parton inputs and conserved order by order in α_S for evolution.

$$\int_0^1 u_V(x)\,dx = 2 \qquad \int_0^1 d_V(x)\,dx = 1$$

i.e. conservation of number of valence quarks.

Also conservation of momentum carried by partons

$$\int_0^1 x\Sigma(x) + xg(x)\,dx = 1.$$

Important constraint on form of gluon which is only probed indirectly.

In determining partons need to consider that not only are there 6 different combinations of partons, but also wide distribution of x from 0.75 to 0.00003. Need many different types of experiment for full determination.

Large x

Quark distributions are determined mainly by structure functions. Dominated by non-singlet valence distributions. Very unlikely to find sea quarks or gluon as $x \rightarrow 1$.

Simple evolution of non-singlet distributions and conversion to structure function

$$\begin{aligned} \frac{d\tilde{f}^{NS}(x,Q^2)}{d\ln Q^2} &= P^{NS}(x,\alpha_s(Q^2)) \otimes \tilde{f}^{NS}(x,Q^2) \\ F_2^{NS}(x,Q^2) &= C^{NS}(x,\alpha_s(Q^2)) \otimes \tilde{f}^{NS}(x,Q^2,\alpha_s(Q^2)) \end{aligned}$$

So evolution of high x structure functions good test of theory and of $\alpha_S(Q^2)$.

However - perturbation theory involves contributions to coefficient function $\sim \alpha_S^n(Q^2)\ln^{2n-1}(1-x)$ and higher twist known to be enhanced as $x \rightarrow 1$. Hence cut $W^2 = Q^2(1/x-1)+m_p^2$ at somewhere in region $10-15\mathrm{GeV}^2$ to avoid contamination of perturbation theory.

Consider charged lepton proton scattering

$$\frac{d^2\sigma}{dxdQ^2} = \frac{2\pi\alpha_2}{Q^4}[(1+(1-y)^2)F_2(x,Q^2) - y^2 F_L(x,Q^2)]$$

ignoring W and Z exchange (small correction for HERA data), and where $y = Q^2/xs$. Both $F_L(x,Q^2)$ and y usually small ($F_L(x,Q^2) = 0$ in simple quark model) so cross-section effectively measure of $F_2(x,Q^2)$.

$$\begin{aligned} F_2^p(x) &\approx x[4/9(u+\bar{u}+c+\bar{c}) + 1/9(d+\bar{d}+s+\bar{s})] \\ F_2^d(x) &\approx x[4/9(d+\bar{d}+c+\bar{c}) + 1/9(u+\bar{u}+s+\bar{s})] \end{aligned}$$

So SLAC, BCDMS NMC data on $F_2^p(x,Q^2)$ and NMC data on $F_2^d(x,Q^2)$ and $F_2^n(x,Q^2)/F_2^p(x,Q^2)$ help determine high x parton distributions dominated by valence quarks.

Also use CCFR and NuTeV charged-current (neutrino) DIS data

$$\begin{aligned}\frac{d^2\sigma^{\nu,\bar{\nu}}}{dxdQ^2} &\propto F_2^{\nu,\bar{\nu}}(x,Q^2)\left[(1-y)+\frac{y^2}{2(1+R(x,Q^2))}\right]\\ &\pm xF_3^{\nu,\bar{\nu}}(x,Q^2)y(1-y/2),\end{aligned}$$

where $R = F_L/(F_2 - F_L)$ and F_3 appears due to parity violation. For the proton

$$\begin{aligned}F_2^{\nu} &= 2x[d+s+\bar{u}+\bar{c}]\\ F_2^{\bar{\nu}} &= 2x[u+c+\bar{d}+\bar{s}]\\ xF_3^{\nu} &= 2x[d+s-\bar{u}-\bar{c}]\\ xF_3^{\bar{\nu}} &= 2x[u+c-\bar{d}-\bar{s}].\end{aligned}$$

Therefore

$$\begin{aligned}F_2^{\nu}+F_2^{\bar{\nu}} &= 2x\sum_i(q+\bar{q}) = \Sigma\\ F_3^{\nu}+F_3^{\bar{\nu}} &= u_V+d_V.\end{aligned}$$

In fact for an iso-scalar target, e.g. iron which is used by CCFR and NuTeV,

$$
\begin{aligned}
F_2^{\nu} &= F_2^{\bar{\nu}} = x\Sigma \\
xF_3^{\nu} &= x(u_V + d_V) + 2x[s - \bar{c}] \\
xF_3^{\bar{\nu}} &= x(u_V + d_V) - 2x[s - \bar{c}].
\end{aligned}
$$

And we must also correct for nuclear shadowing effects. (Parton distributions in nucleons in nuclei not the same as for free nucleons. Also applied for deuterium data.)

Comparison between theory and data good, and leads to determination of valence quarks at high x.

Also some HERA charged current-data at high Q^2 gives potential information on flavour decomposition. Currently low statistics. Improving.

Find that at large x $u_V(x) > d_V(x)$, and that $xq_V(x) \sim (1-x)^3$, but no constraint in limit $x \to 1$. Some theory suggests $d_V(x)/u_V(x) \to$ constant as $x \to 1$, but no real evidence for or against.

Description of large x BCDMS and SLAC measurements of F_2^p.

High-x partons evolve through splitting to smaller x partons.

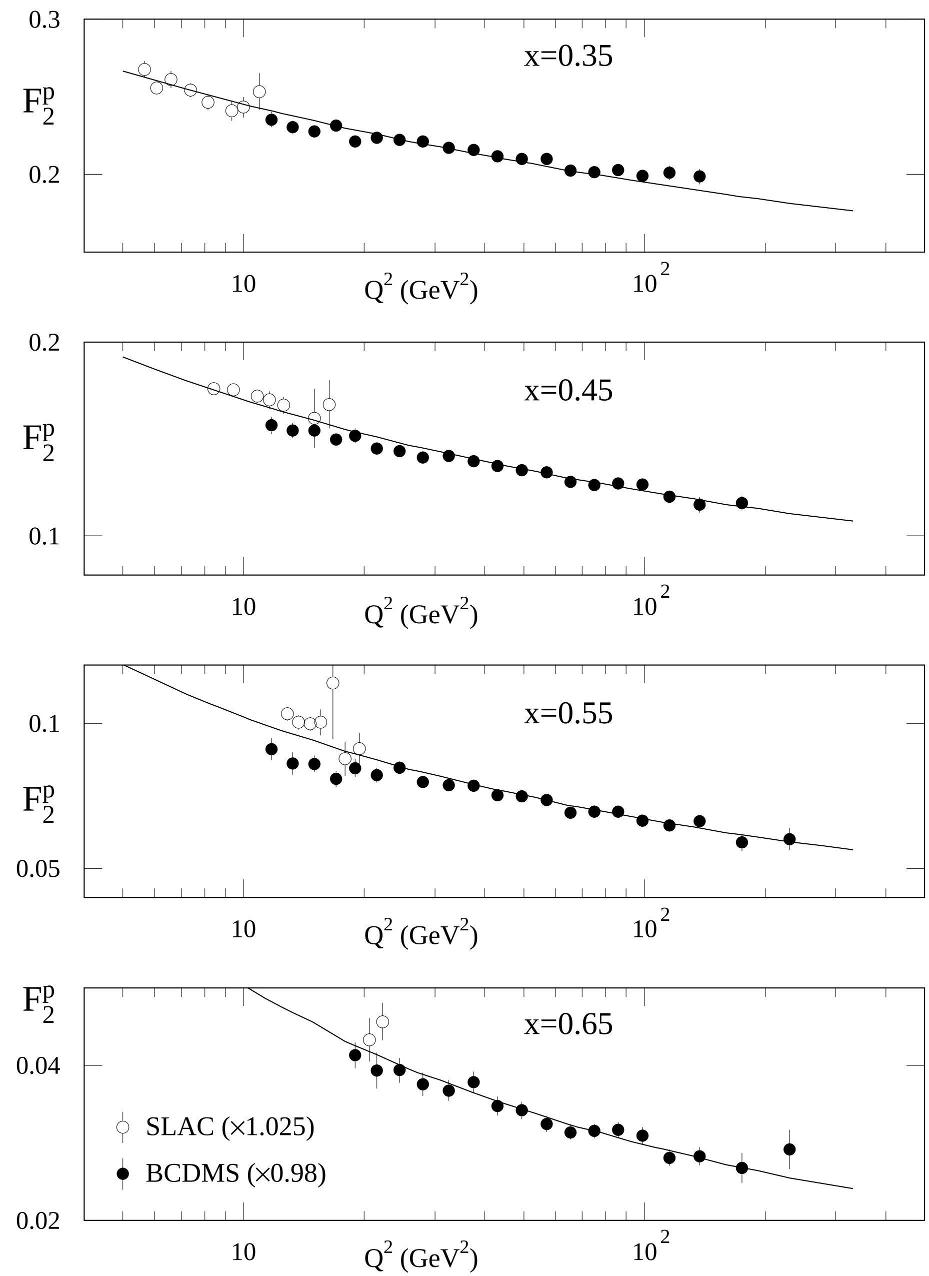

Description of large x NMC measurements of F_2^n/F_2^p.

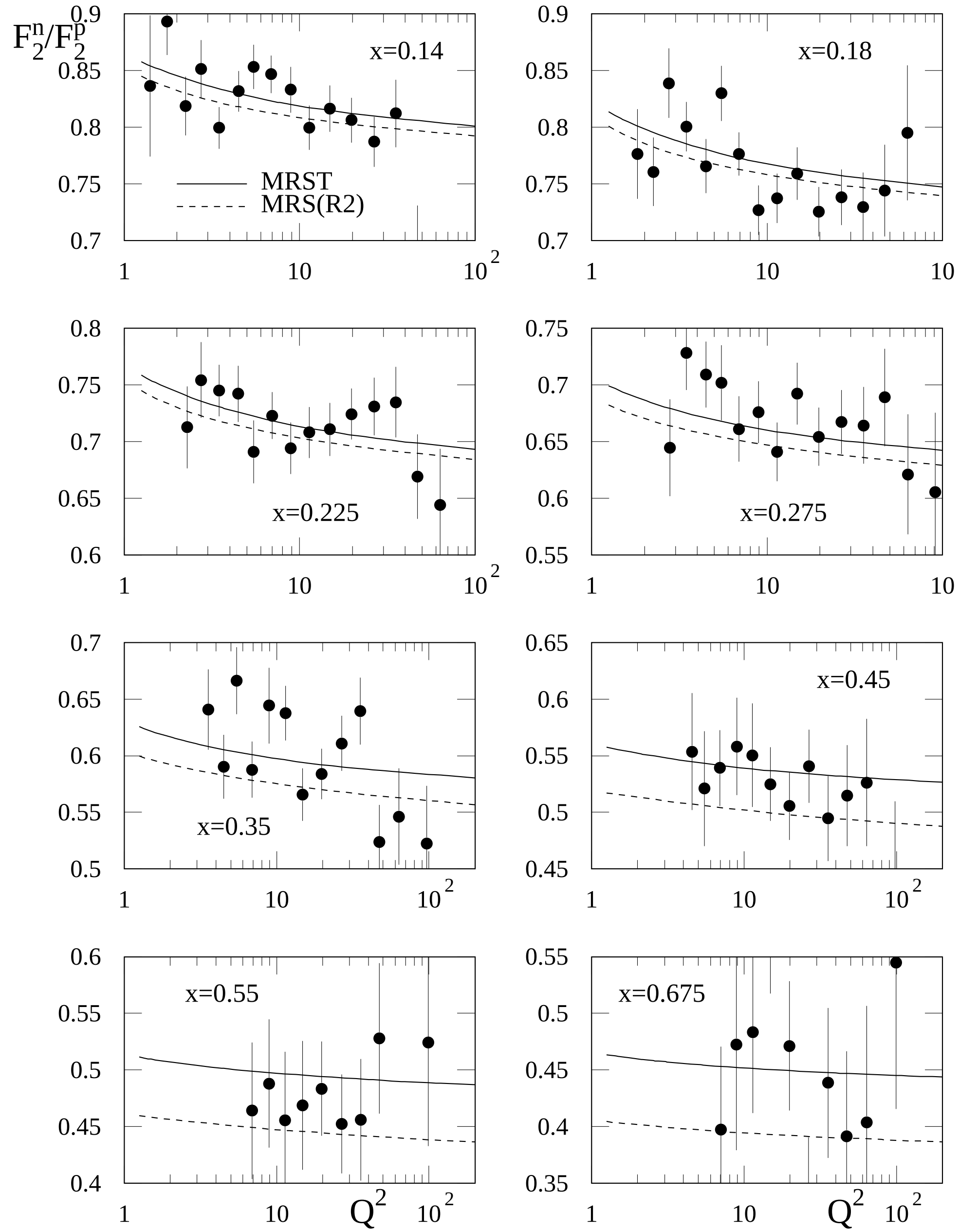

Description of large x CCFR measurements of $F_3^{\nu N}$.

See fixed point at about $x = 0.14$.

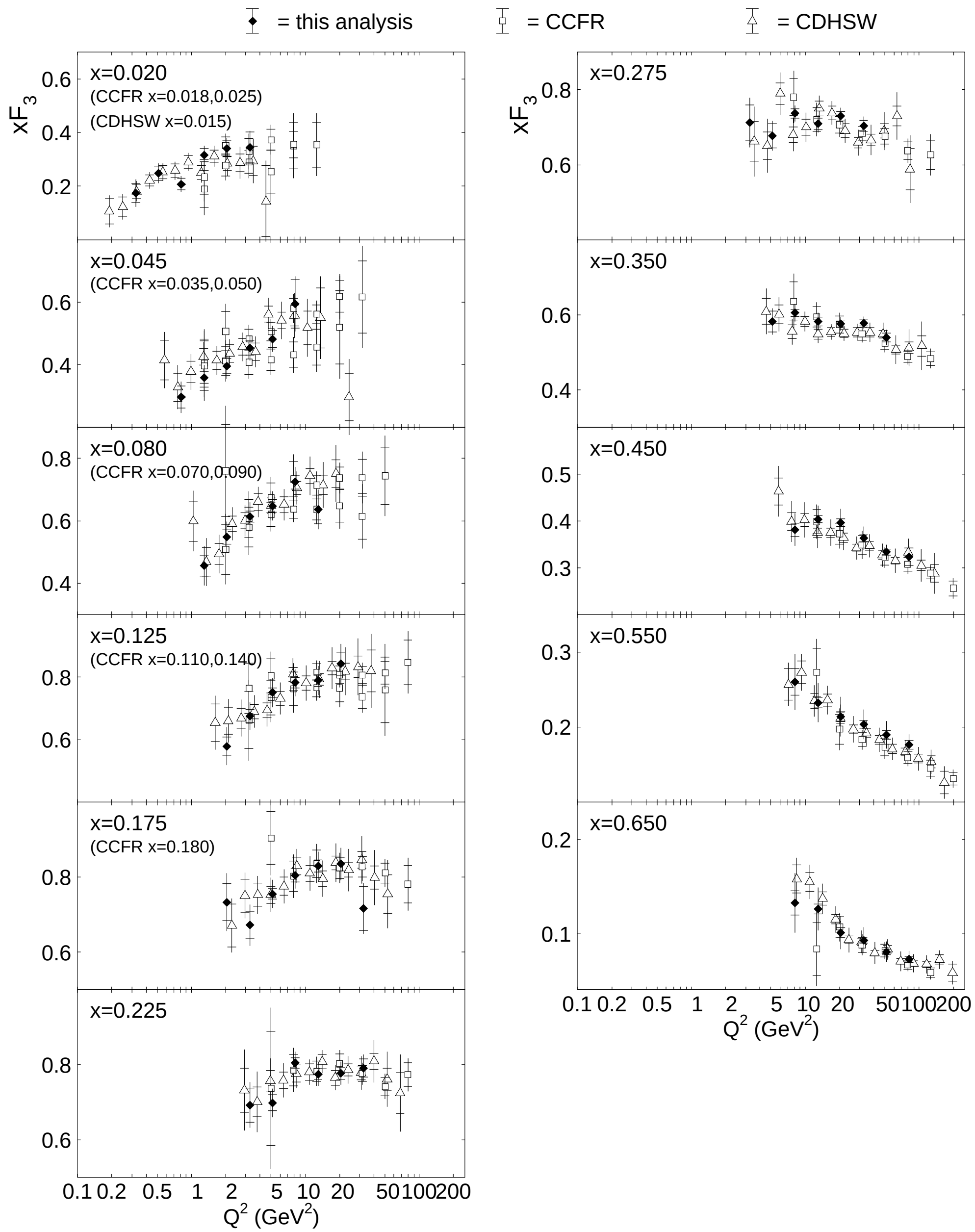

As x decreases the sea quarks become more important. These are determined at $x \sim 0.2$ by Drell-Yan scattering at Fermilab (E605, E772, E866). Process is production of lepton pairs from quark-antiquark annihilation in proton-proton scattering.

$x_F = x_1 - x_2$ and $\tau = x_1 x_2 = M^2/s$.

$$\frac{d\sigma}{dM^2 dx_F} \propto \sum e_q^2 (q(x_1)\bar{q}(x_2) + q(x_2)\bar{q}(x_1)).$$

Probe of $\bar{u}$ and $\bar{d}$ in the proton at moderate x. Find $\bar{q} \sim (1-x)^7$.

Very recently include Z-production data from Tevatron which probes smaller x.

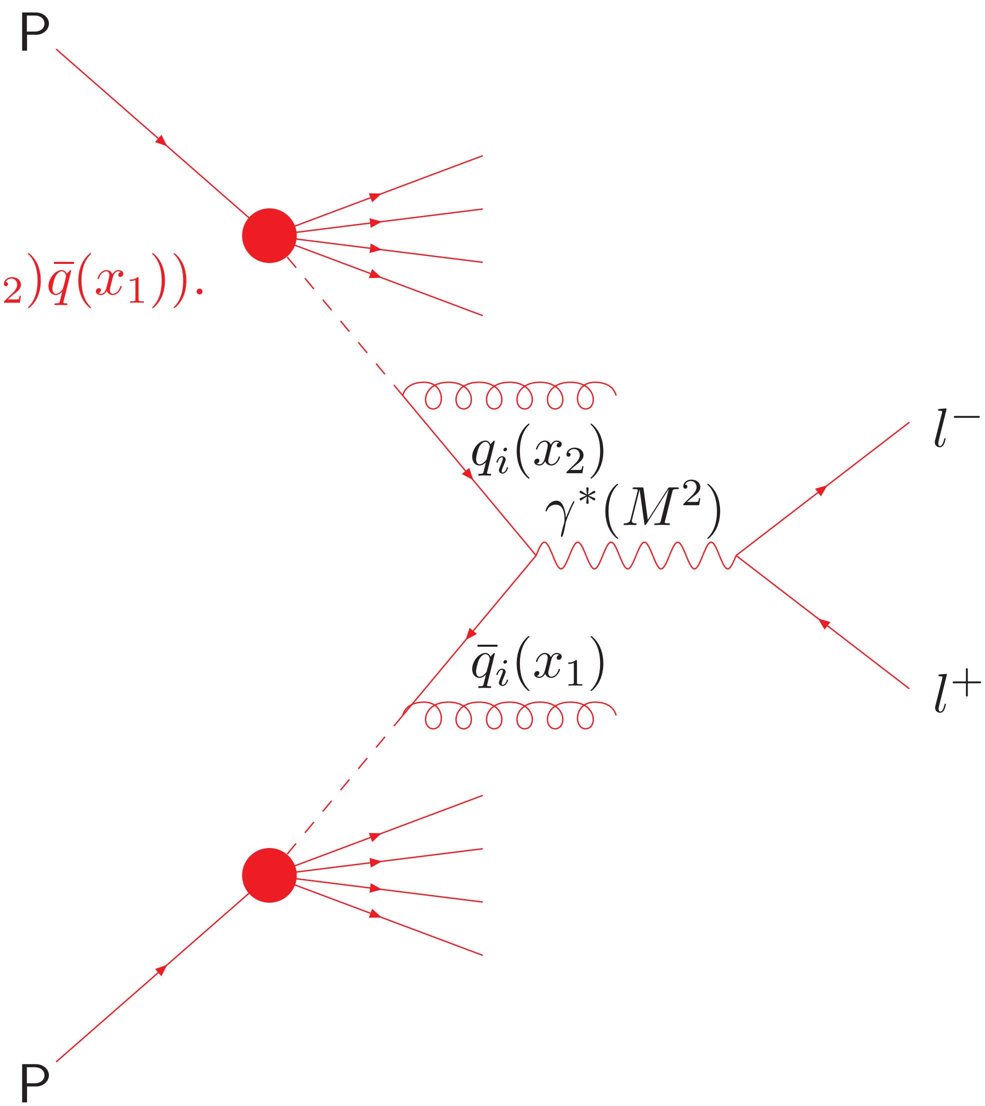

Description of Drell-Yan scattering.

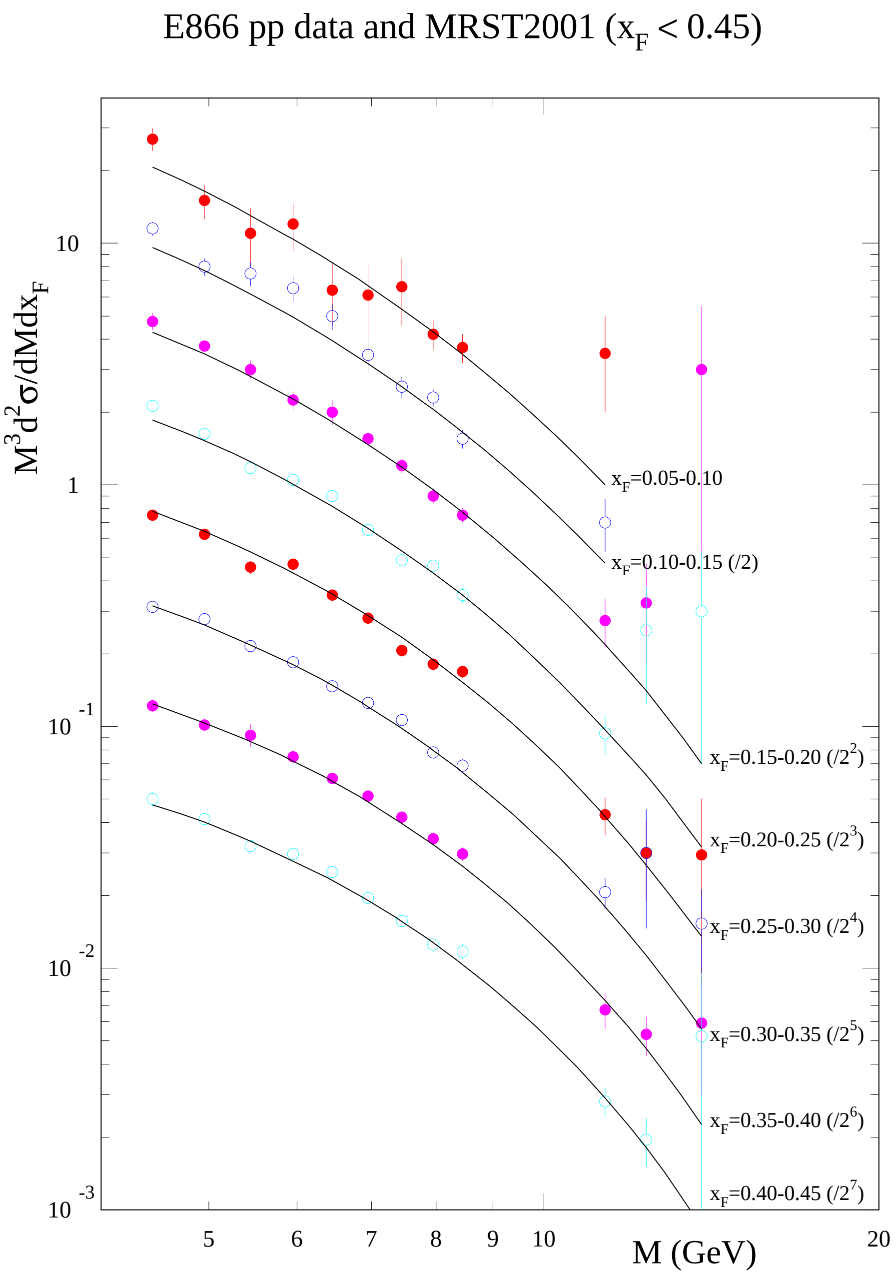

Description of Drell-Yan scattering.

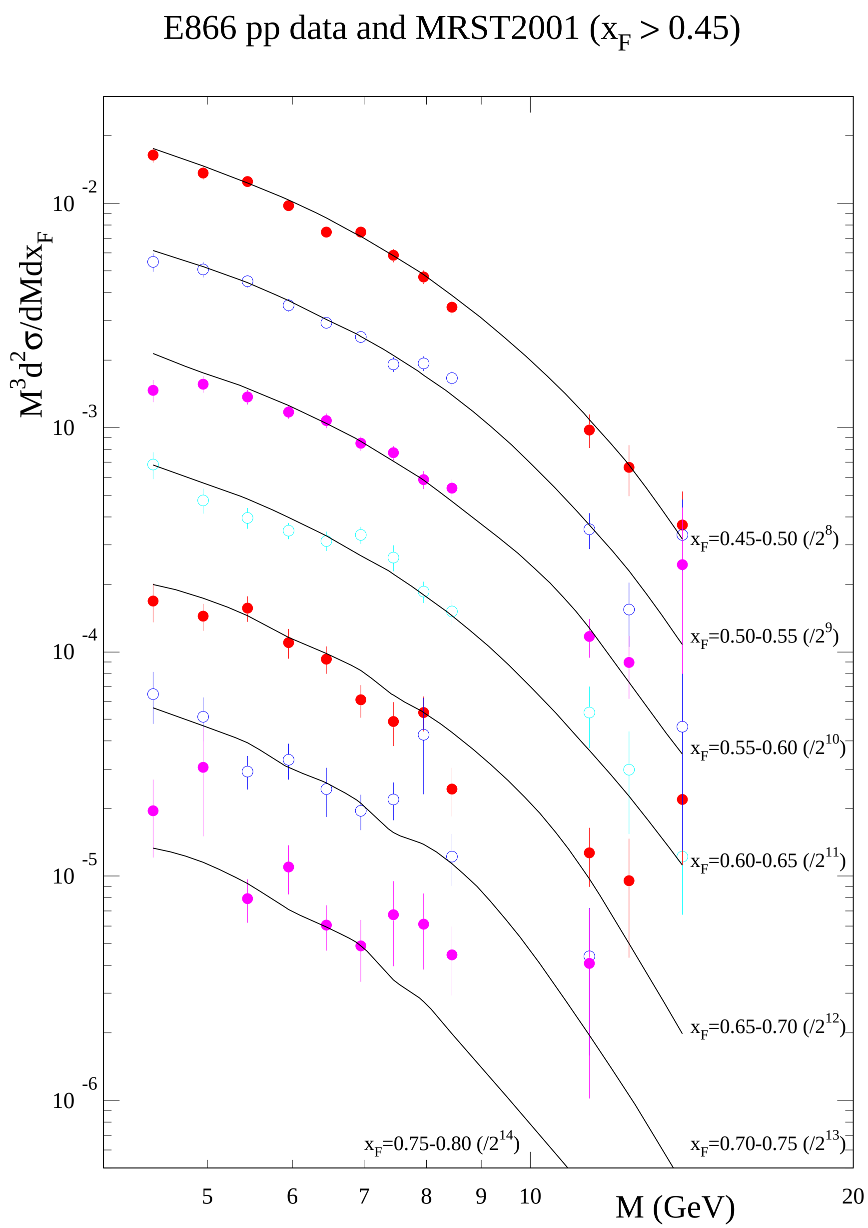

Can look at same thing at the Tevatron for the Z rapidity distribution, which depends on weak couplings of quarks rather than electromagnetic.

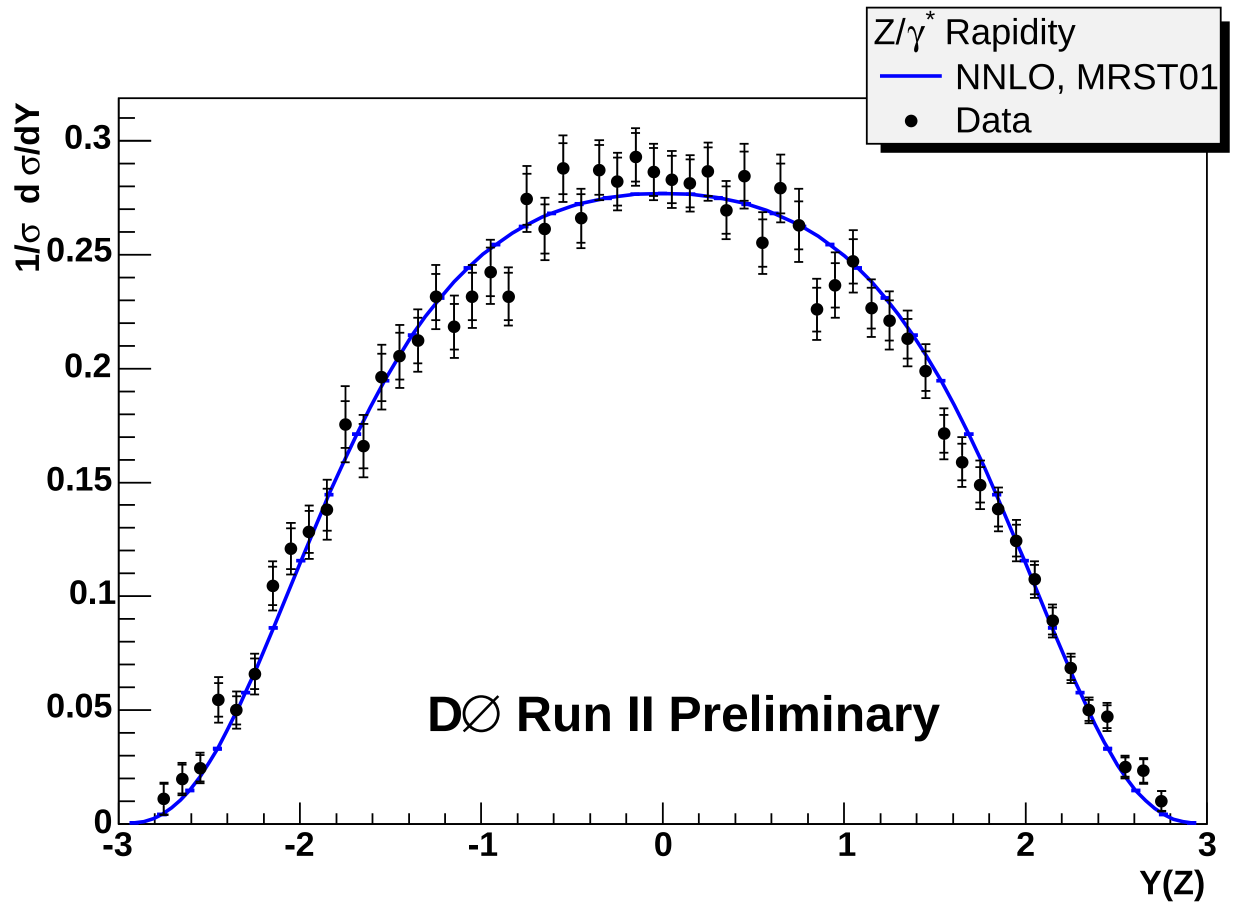

$y = 1/2 \ln\left(\frac{(E+p_z)}{(E-p_z)}\right)$, i.e. how far forward/back in the detector the Z boson is.

Also need to consider the precise difference between $\bar{u}$ and $\bar{d}$. Related to Gottfried sum rule.

$$I_{GS} = \int_0^1 \frac{dx}{x}(F^{\mu p} - F^{\mu n}) = \frac{1}{3}\int_0^1 dx(u_V - d_V + 2(\bar{u} - \bar{d}))$$
$$= \frac{1}{3} + \frac{2}{3}\int_0^1 dx(\bar{u} - \bar{d})$$

This was measured by NMC to be 0.235 ± 0.026 which implies $\int dx(\bar{d} - \bar{u}) \approx 0.1$.

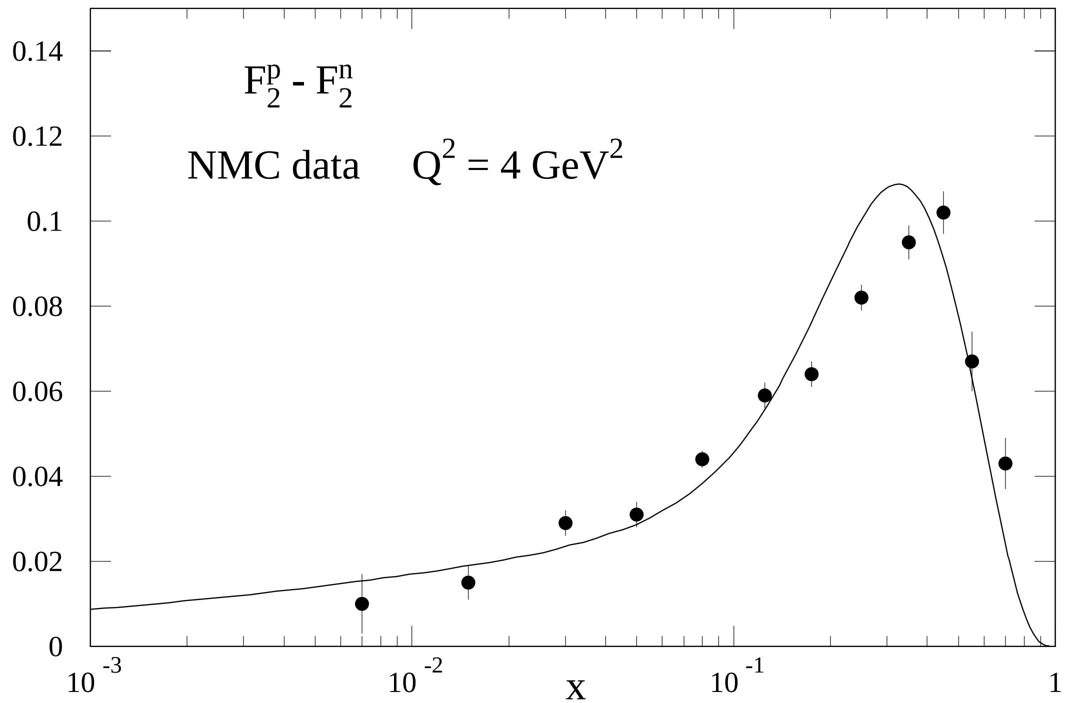

Information more directly available from Drell-Yan asymmetry

$$A_{DY} = \frac{\sigma_{pp} - \sigma_{pn}}{\sigma_{pp} + \sigma_{pn}} = \frac{1-r}{1+r},$$

where

$$r \approx \frac{4u_1\bar{d}_2 + d_1\bar{u}_2 + 4\bar{u}_1 d_2 + \bar{d}_1 u_2}{4u_1\bar{u}_2 + d_1\bar{d}_2 + 4\bar{u}_1 u_2 + \bar{d}_1 d_2},$$

and 1 labels the proton and 2 the neutron.

In fact measure the quantity

$$R_{dp} = \frac{\sigma_{pd}}{2\sigma_{pp}} = \frac{1}{2}(1+r),$$

which contains the same information.

E866 measured very accurately from $0.04 < x < 0.3$. Gives clear evidence of $\bar{u} - \bar{d}$ asymmetry, but not as much as suggested previously.

Seems to reach maximum at $x \approx 0.2$. Not clear what happens as $x \to 1$.

Drell-Yan asymmetry compared to E866 data.

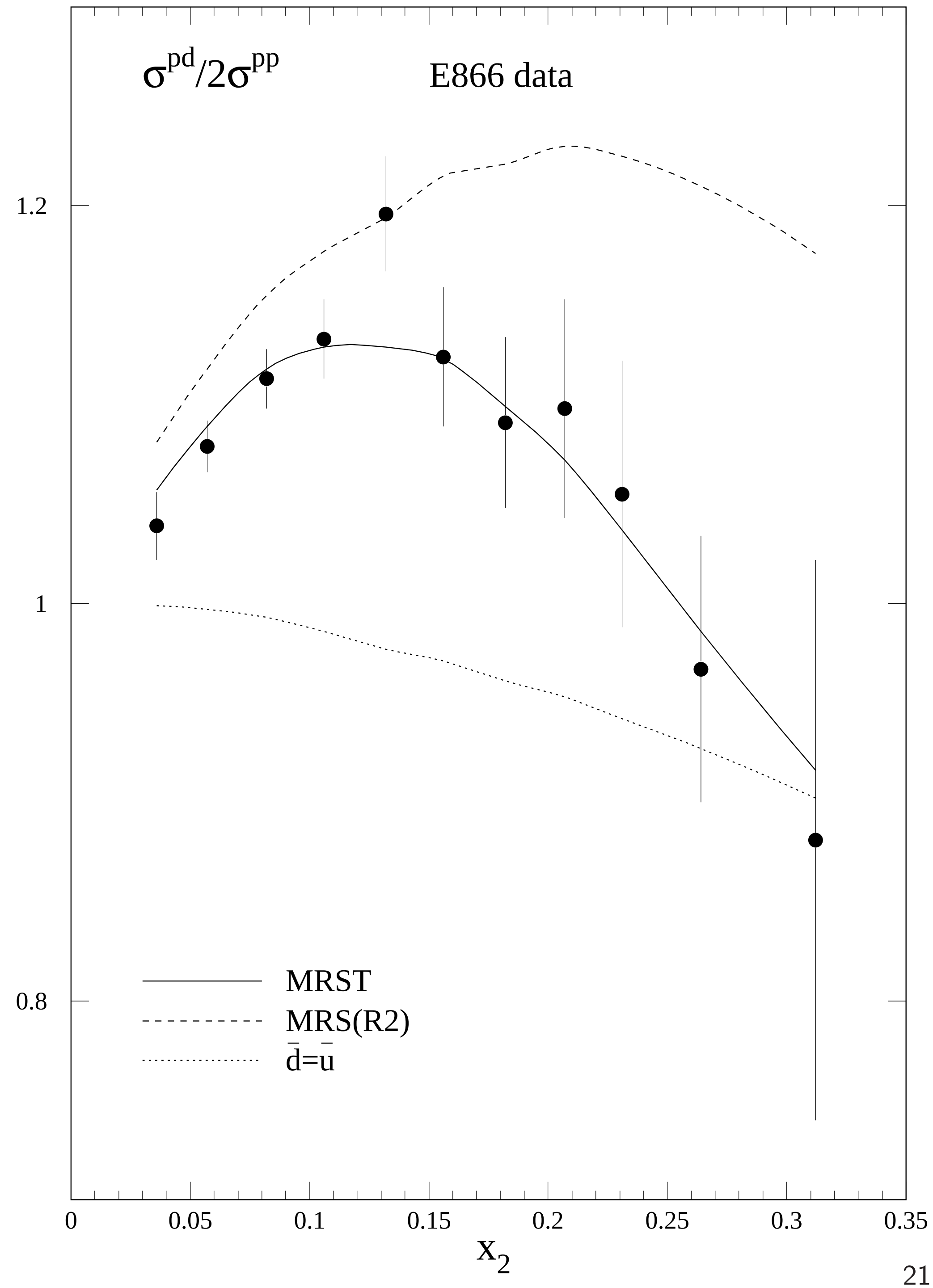

It is now possible to find the strange quark distribution directly. This is done using unlike sign dimuon production at CCFR and NuTeV, i.e.

$$\nu_\mu \to \mu^- + W^+$$

followed by

$$W^+ + s \to c \to D^+ \to \mu^+.$$

or for antineutrinos

$$\bar{\nu}_\mu \to \mu^+ + W^-$$

followed by

$$W^- + \bar{s} \to \bar{c} \to D^- \to \mu^-.$$

In Global fits it was previously assumed that at Q_0^2 we have $s(x) = \kappa 0.5(\bar{u} + \bar{d})$. Using $Q_0^2 = 1\mathrm{GeV}^2$ and $\kappa = 0.4$ works very well, i.e. strange is 18% of the input sea. Since all quarks evolve equally this fraction increases as Q^2 increases.

Can now do better and get shape of strange distribution. Also some evidence $s(x) \neq \bar{s}(x)$.

NuTeV $\frac{100\pi}{G_F^2 M_N E_\nu}\frac{d\sigma}{dxdy}(\nu_\mu N \to \mu^+\mu^- X)$ in GeV^{-2}, $\chi^2 = 11/21$ DOF

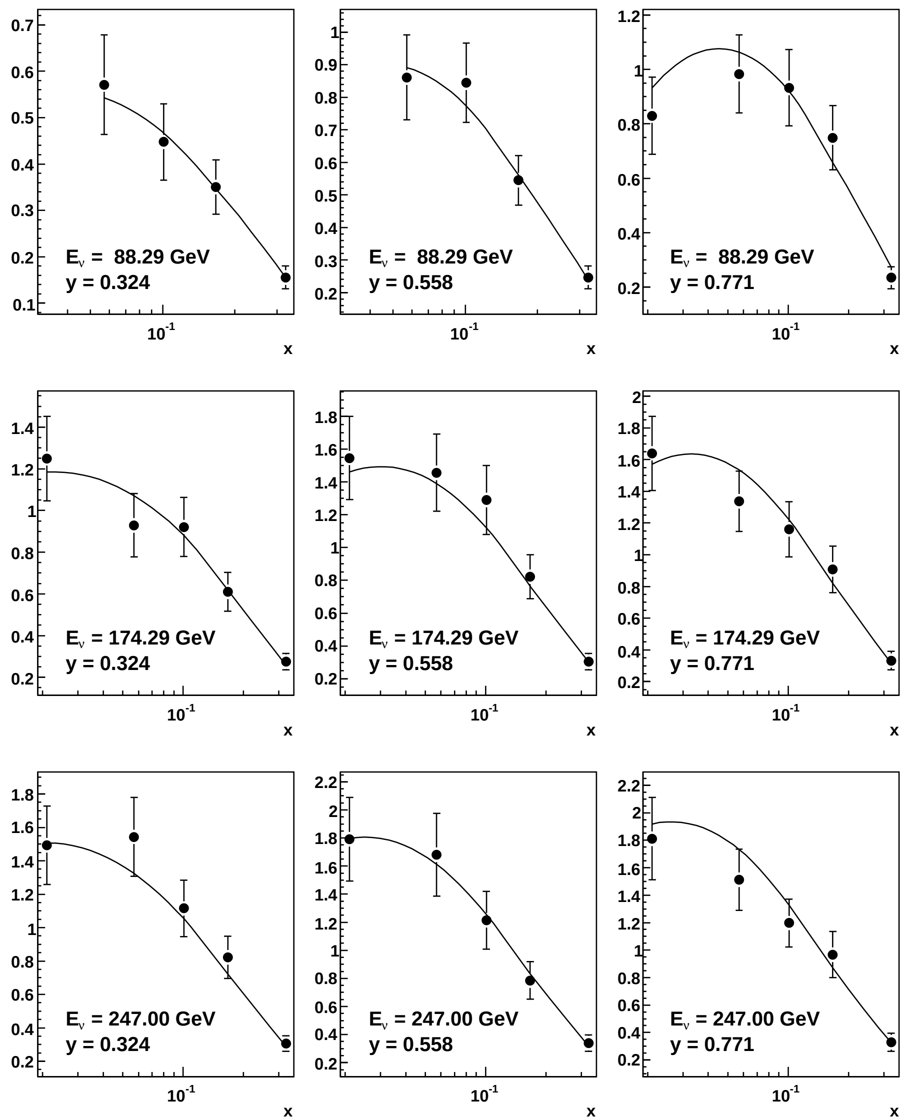

NuTeV $\frac{100\pi}{G_F^2 M_N E_{\bar\nu}}\frac{d\sigma}{dxdy}(\bar\nu_\mu N \to \mu^+\mu^- X)$ in GeV^{-2}, $\chi^2 = 27/19$ DOF

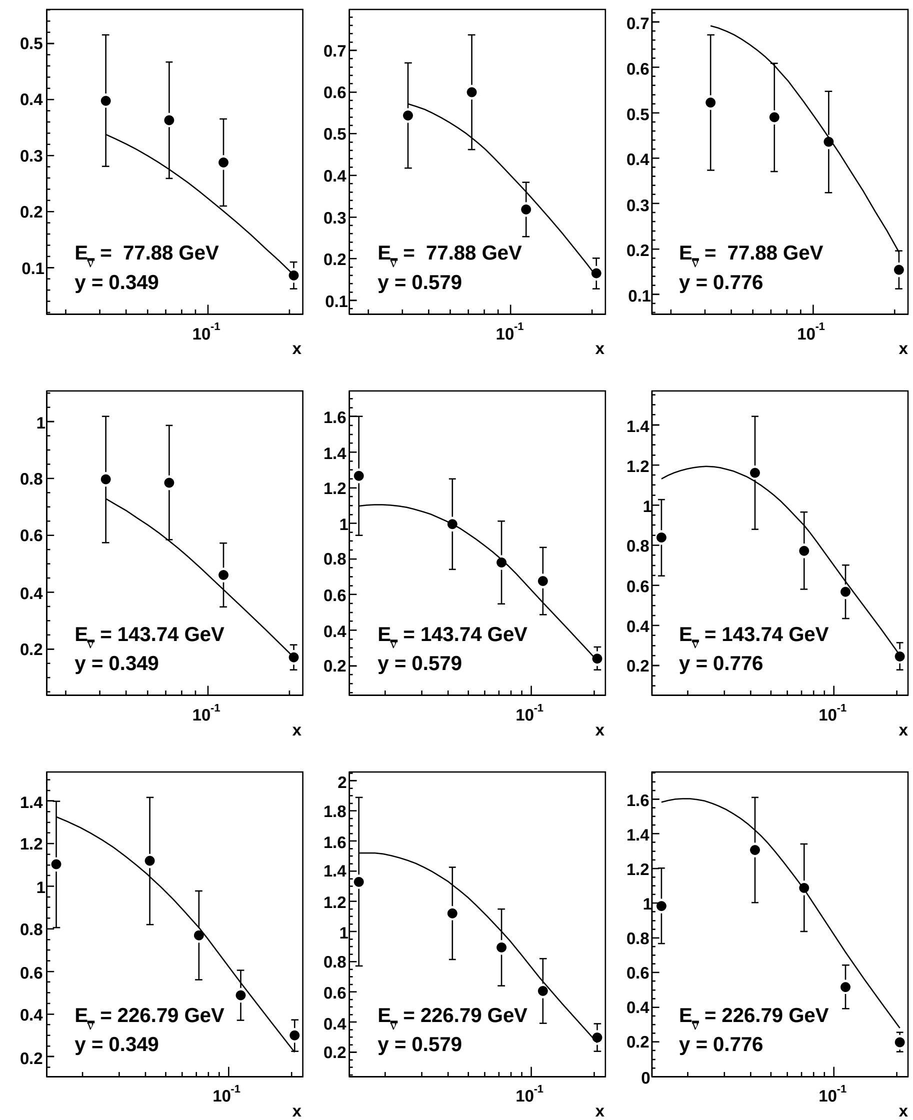

Find reduced ratio of strange to non-strange sea compared to previous default $\kappa = 0.5$.

Suppression at high x, i.e. low W^2. Effect of m_s?

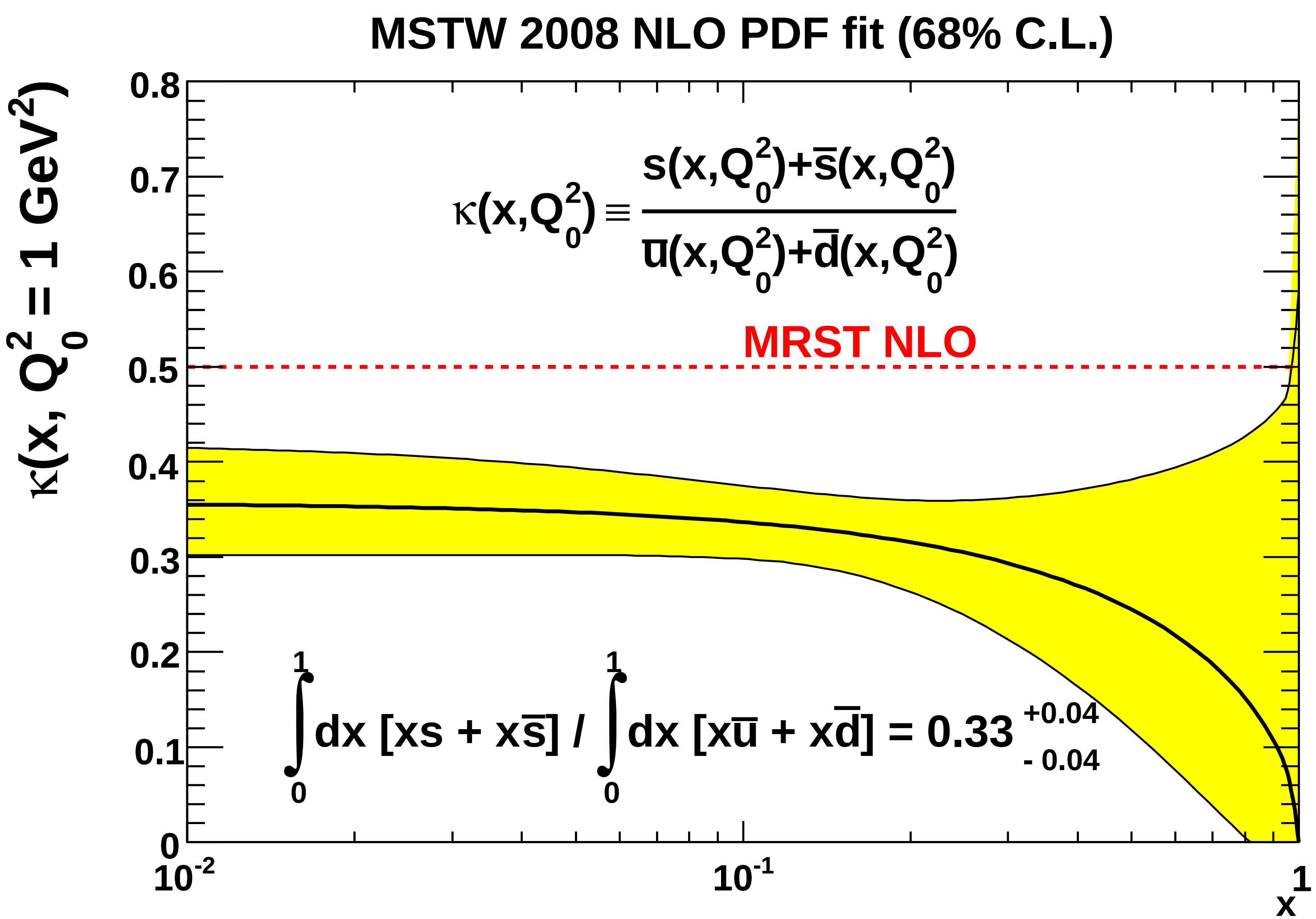

Fit to strange and antistrange separately.

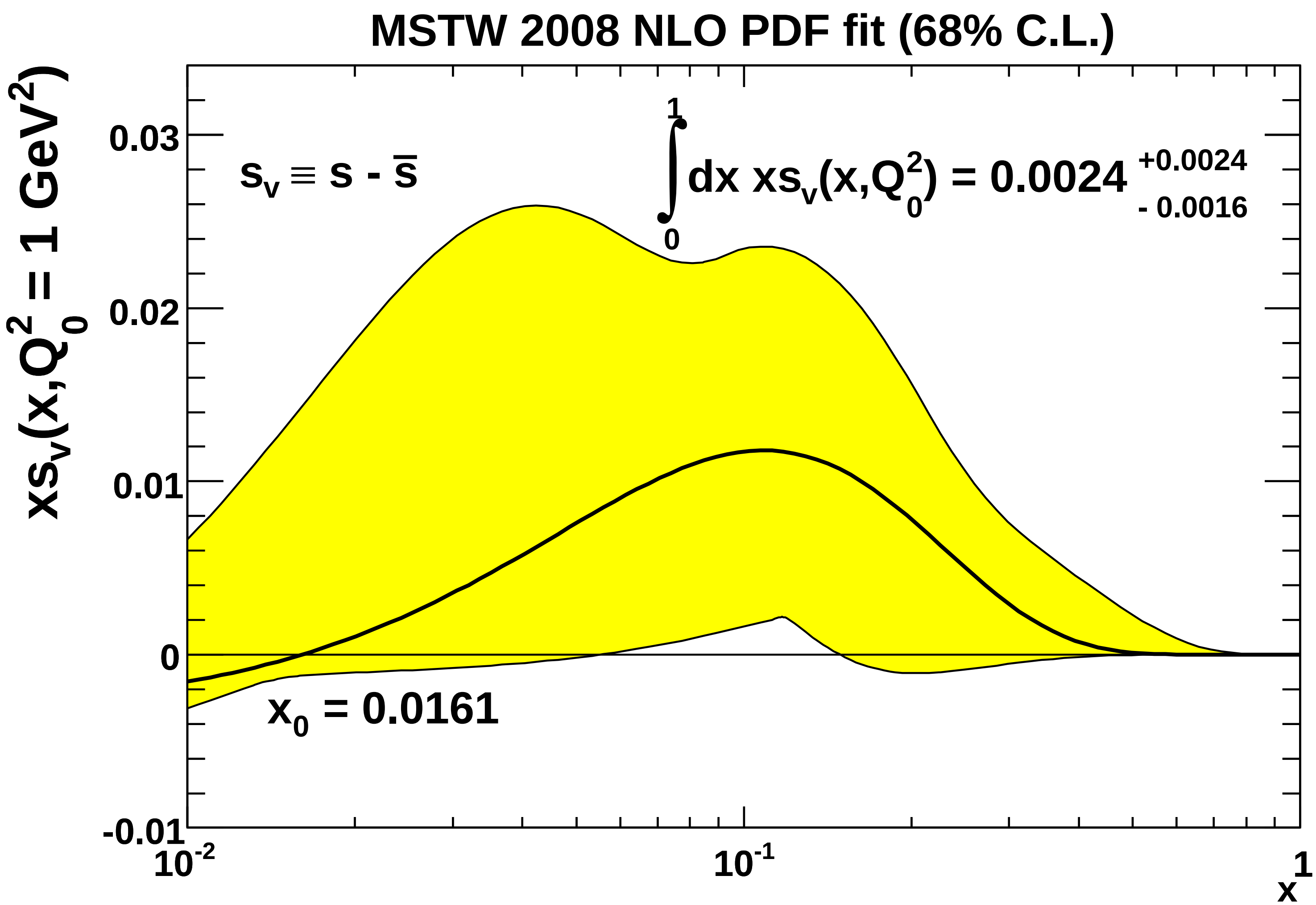

The final piece of information on the light quarks at moderate to large x comes from W- or lepton asymmetry at the Tevatron $p\bar{p}$ collider.

$$A_W(y) = \frac{d\sigma(W^+)/dy - d\sigma(W^-)/dy}{d\sigma(W^+)/dy + d\sigma(W^-)/dy}$$
$$\approx \frac{u(x_1)d(x_2) - d(x_1)u(x_2)}{u(x_1)d(x_2) + d(x_1)u(x_2)},$$

where $x_{1,2} = x_0 \exp(\pm y), \quad x_0 = \frac{M_W}{\sqrt{s}}$.

Since $u(x) > d(x)$ at large x, whereas they become roughly equal at smaller x, $A_W(y)$ is positive for $x_1 > x_0 = 0.05$ $(y > 1)$ where measurements are taken.

This helps pin down the u and d quarks in the region $x \sim 0.1$ as well as giving compatible information to NMC and CCFR/NuTeV at higher x and thus contributes to the determination of the two valence quark distributions.

In practice it is the final state leptons that are detected, so it is really the lepton asymmetry

$$A(y_l) = \frac{\sigma(l^+) - \sigma(l^-)}{\sigma(l^+) + \sigma(l^-)}$$

which is measured.

Comparison of fits to CDF data with various partons.

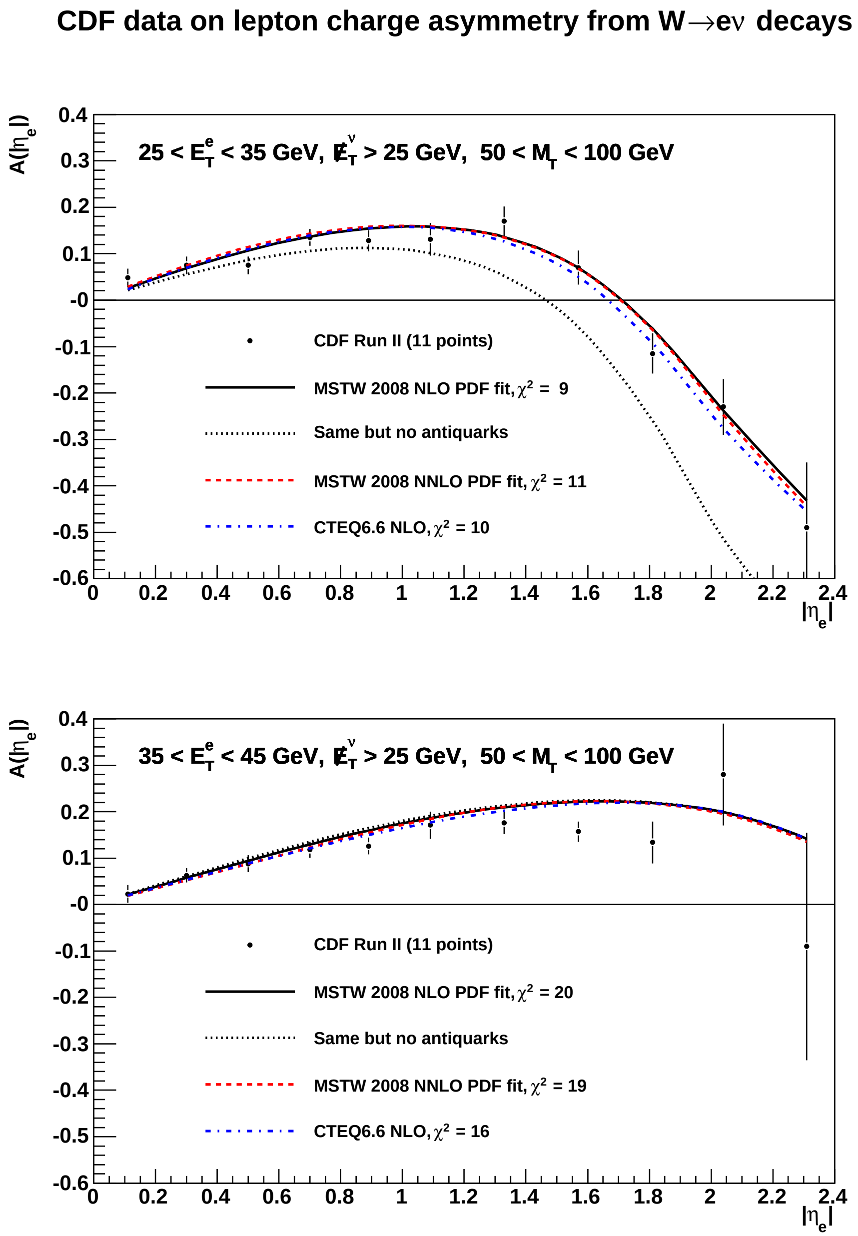

Same idea at the LHC, but this time a pp collider and $x > 0.01$.

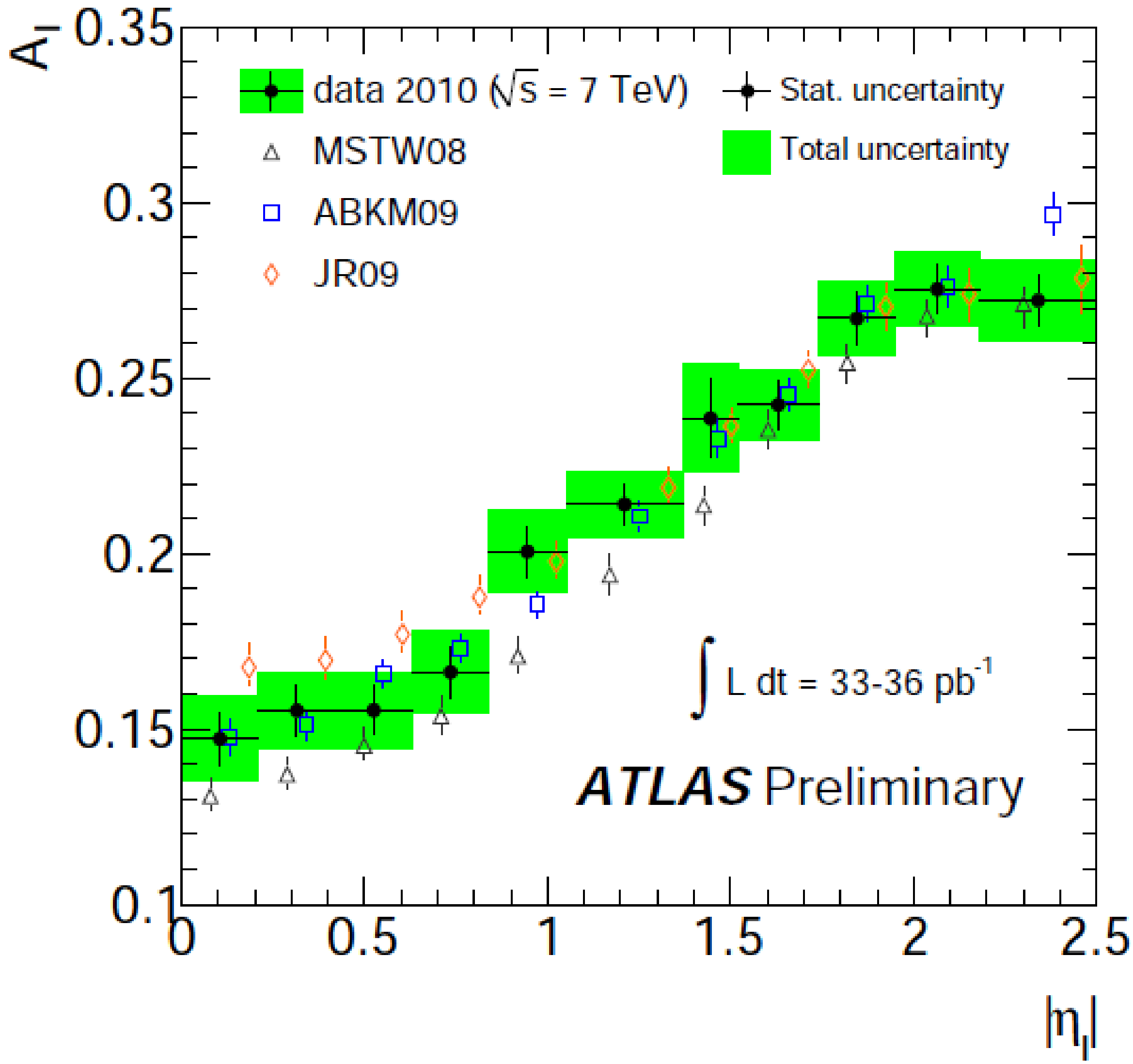

Now no vanishing at $y = 0$.

Can also look at individual rapidity distributions so not lose information which cancels in the ratio

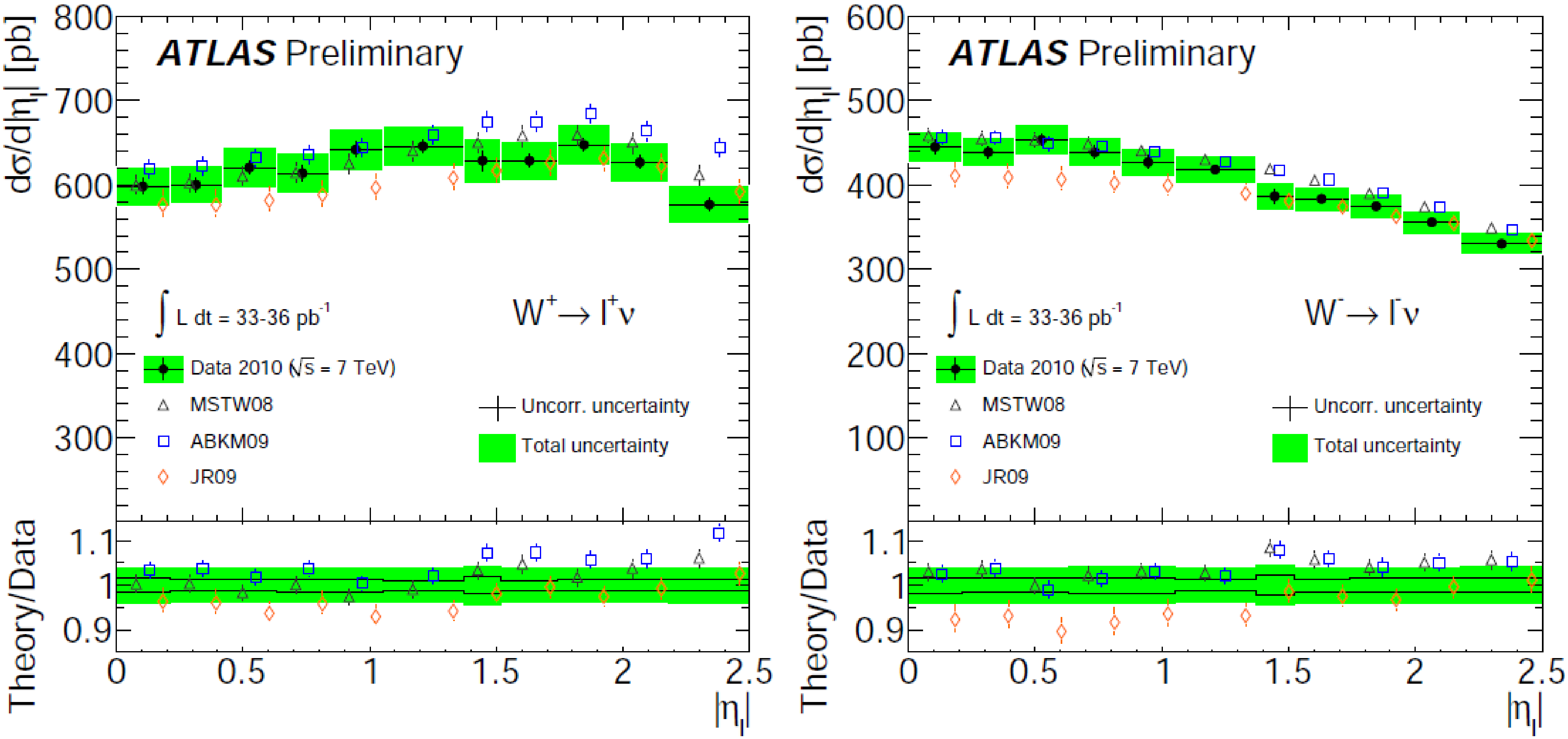

Also good to compare with total cross-sections and ratios.

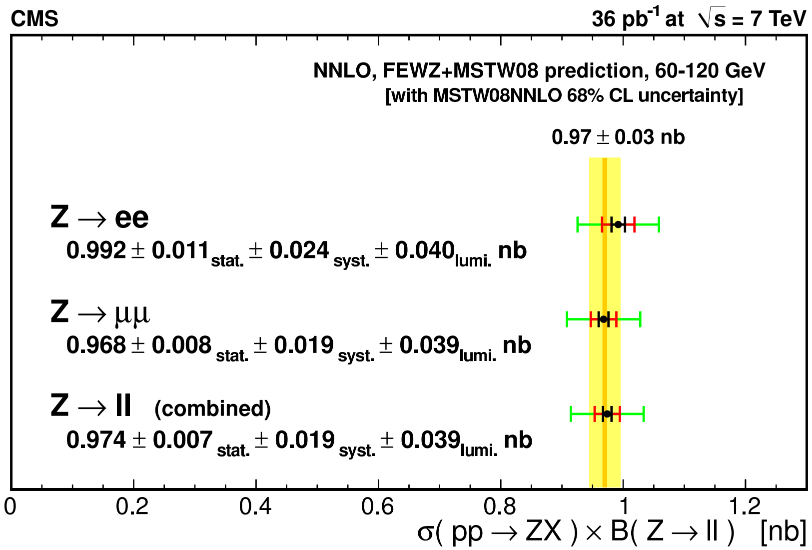

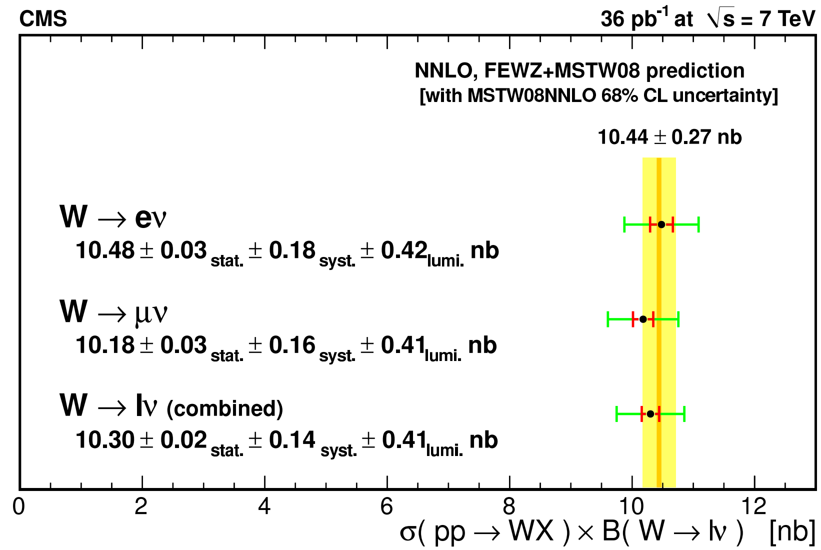

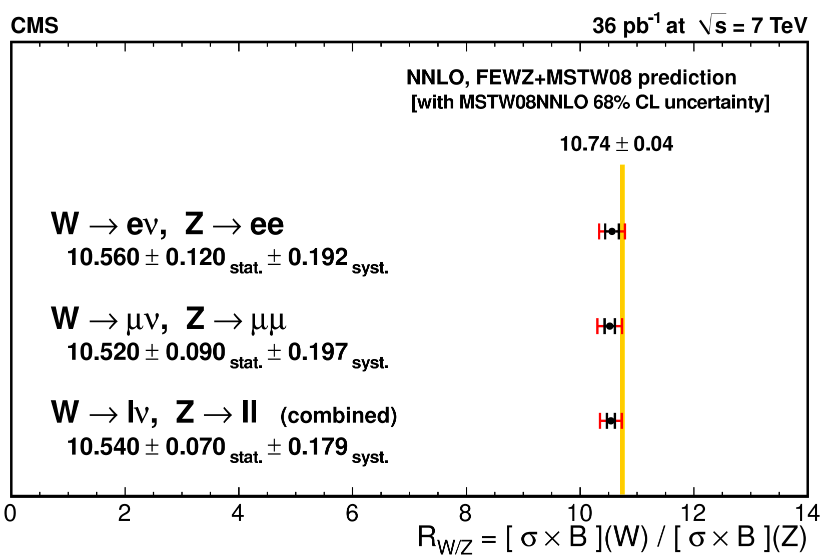

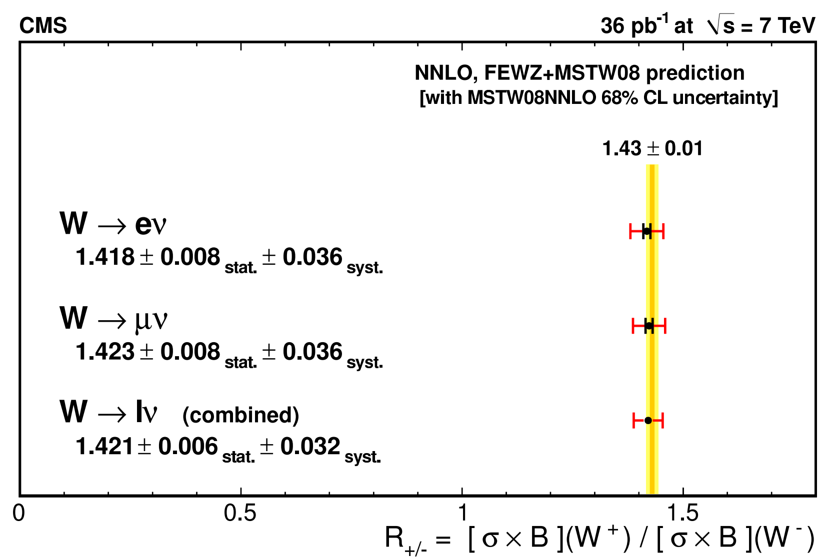

QED –improved DGLAP equations.

$$
\begin{aligned}
\frac{\partial q_i(x,\mu^2)}{\partial \log \mu^2} &= \frac{\alpha_S}{2\pi}\int_x^1 \frac{dy}{y}\left\{P_{qq}(y)\; q_i(\frac{x}{y},\mu^2) + P_{qg}(y,\alpha_S)\; g(\frac{x}{y},\mu^2)\right\} \\
&+ \frac{\alpha}{2\pi}\int_x^1 \frac{dy}{y}\left\{\tilde{P}_{qq}(y)\; e_i^2 q_i(\frac{x}{y},\mu^2) + P_{q\gamma}(y)\; e_i^2 \gamma(\frac{x}{y},\mu^2)\right\} \\
\frac{\partial g(x,\mu^2)}{\partial \log \mu^2} &= \frac{\alpha_S}{2\pi}\int_x^1 \frac{dy}{y}\left\{P_{gq}(y)\; \sum_j q_j(\frac{x}{y},\mu^2) + P_{gg}(y)\; g(\frac{x}{y},\mu^2)\right\} \\
\frac{\partial \gamma(x,\mu^2)}{\partial \log \mu^2} &= \frac{\alpha}{2\pi}\int_x^1 \frac{dy}{y}\left\{P_{\gamma q}(y)\; \sum_j e_j^2\; q_j(\frac{x}{y},\mu^2) + P_{\gamma\gamma}(y)\; \gamma(\frac{x}{y},\mu^2)\right\}
\end{aligned}
$$

at leading order in α_S and α, where

$$
\tilde{P}_{qq} = C_F^{-1} P_{qq}, \qquad P_{\gamma q} = C_F^{-1} P_{gq},
$$

$$
P_{q\gamma} = T_R^{-1} P_{qg}, \qquad P_{\gamma\gamma} = -\tfrac{2}{3}\, \sum_i e_i^2\, \delta(1-x)
$$

and momentum is conserved:

$$
\int_0^1 dx\; x\; \left\{\sum_i q_i(x,\mu^2) + g(x,\mu^2) + \gamma(x,\mu^2)\right\} = 1.
$$

Effect on quark distributions negligible at small x where gluon contribution dominates evolution. Gluon loses a little momentum to photon.

At large x, photon radiation from quarks leads to faster evolution, roughly equivalent to a slight shift in α_S : $\Delta\alpha_S(M_Z^2) \simeq +0.0003$

Photon similar size to b-quark. Bigger at high x.

Overall QED effects much smaller than many sources of uncertainty. Automatically violate isospin though.

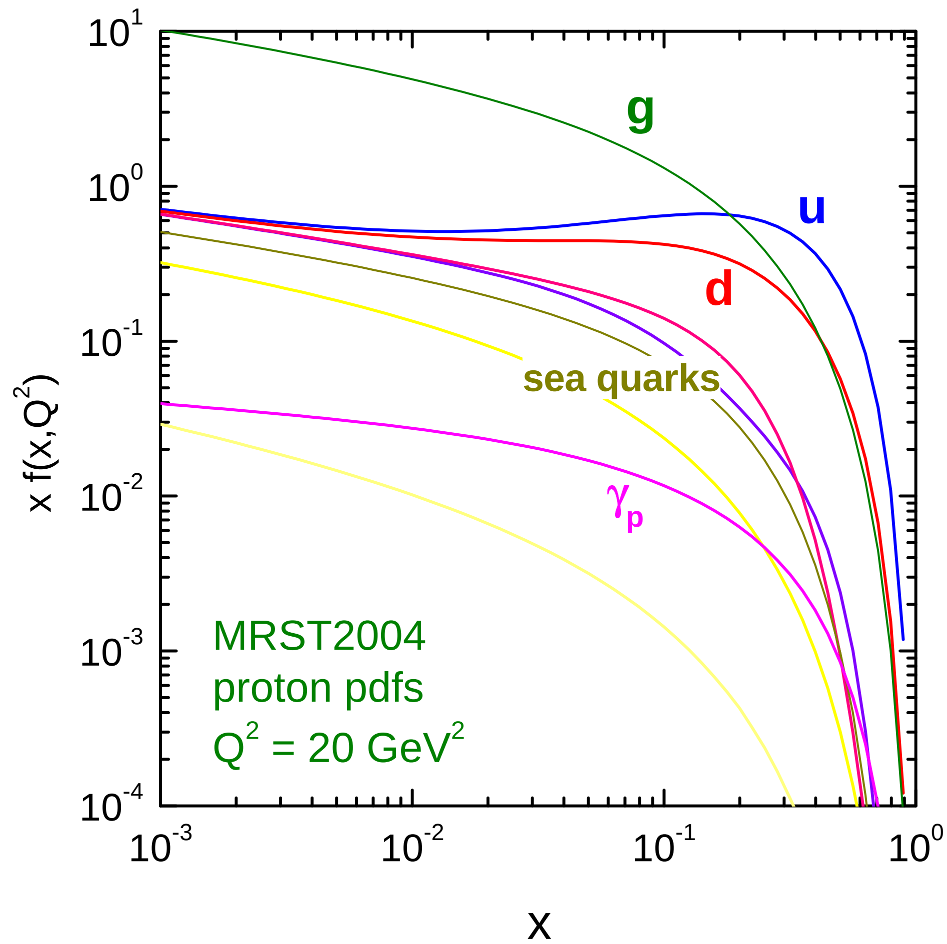

Gluon distribution

The above measurements constrain the high and moderate x quarks to a few percent or better. It is far more difficult to obtain precise information on the form of the high x gluon. Until recently many groups determined the gluon at high x via prompt photon production, e.g.

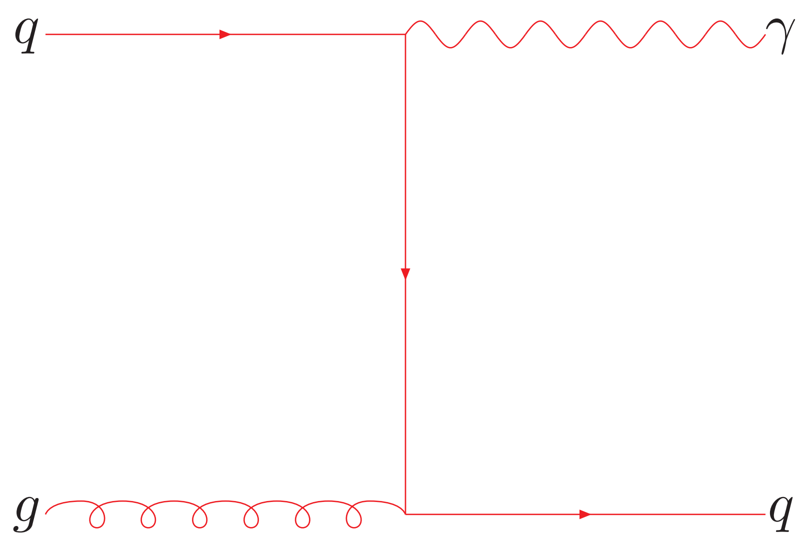

In principle this is a direct test of the large x gluon - $x_T = 2p_T/\sqrt{s}$.

However, $d^2\sigma/dEdp_T$ is sensitive to nonperturbative information about the intrinsic k_T of the gluons in the proton, to resummation of threshold logarithms, i.e. $\ln(1-x_T)$, and to the interplay between the two. Also, some experiments probing similar regions of parameter space give results which are difficult to reconcile. Hence, this gives only a rough indication of the gluon distribution.

Some much higher p_T data from colliders.

Not precise enough to really constraint PDFs.

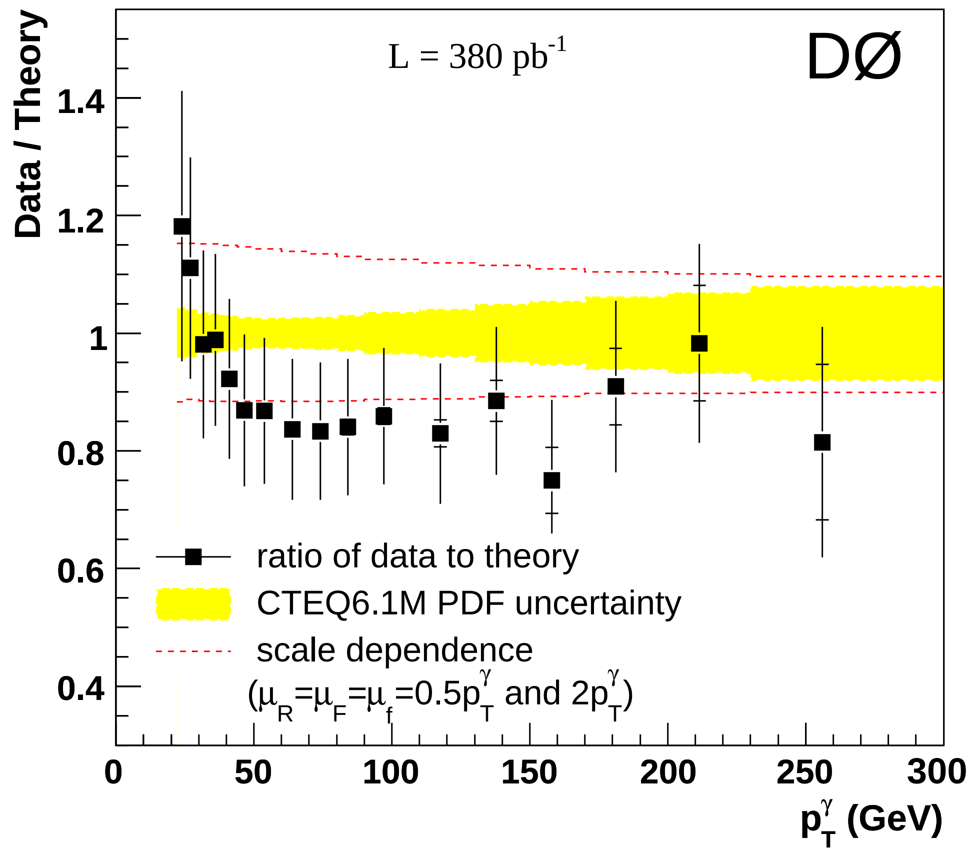

Current best determination of high x gluon distribution given by inclusive jet measurements by D0 and CDF at Tevatron. Measure $d\sigma/dE_T dy$ E_T is the transverse energy of the jet.

$y = \ln((E + p_z)/(E - p_z))$.

For run II measurements in different bins of rapidity for both D0 and CDF. Now also available for ATLAS and CMS. Gives better coverage of x - asymmetric x for incoming partons.

Tevatron data

At central rapidity $x_T = 2E_T/\sqrt{s}$, and measurement extend up to $E_T \sim 400\mathrm{GeV}$, i.e. $x_T \sim 0.45$, and down to $E_T \sim 60\mathrm{GeV}$, i.e. $x_T \sim 0.06$.

At matrix element level gluon-gluon fusion dominates

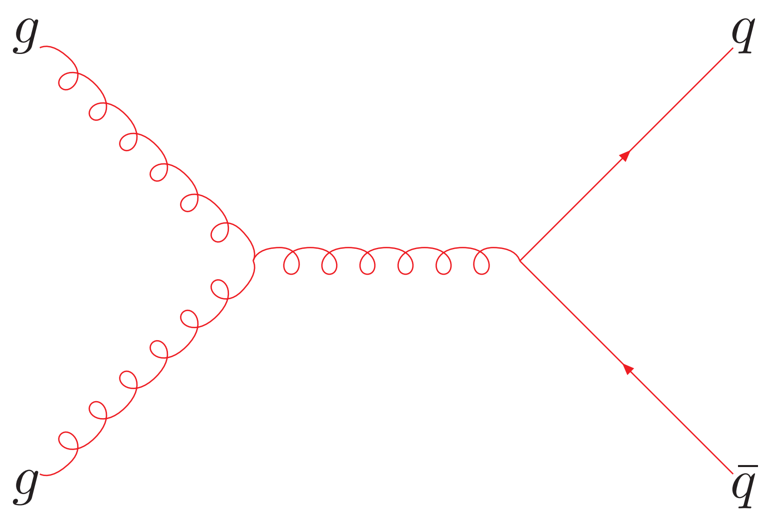

However, the gluon distribution falls off more quickly as $x \to 1$ than quark distributions so there is a transition from gluon-gluon fusion at small x_T, to gluon-quark

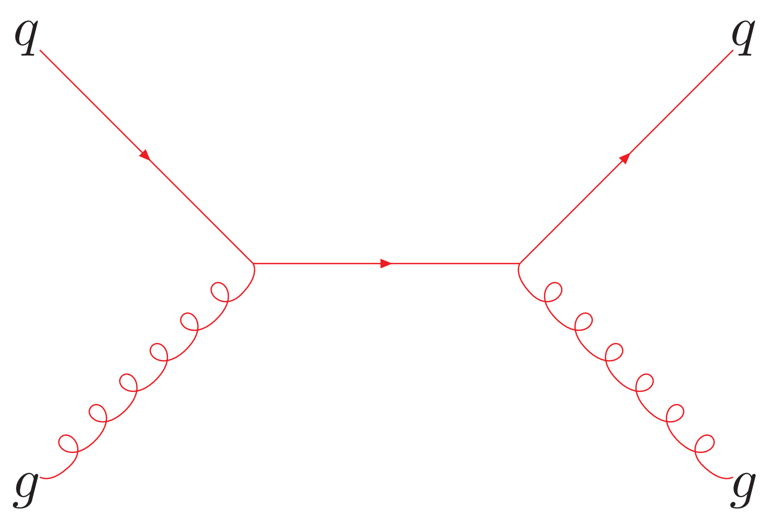

at intermediate x_T to quark-quark at high x_T. However, even at the highest x_T gluon-quark contributions are significant.

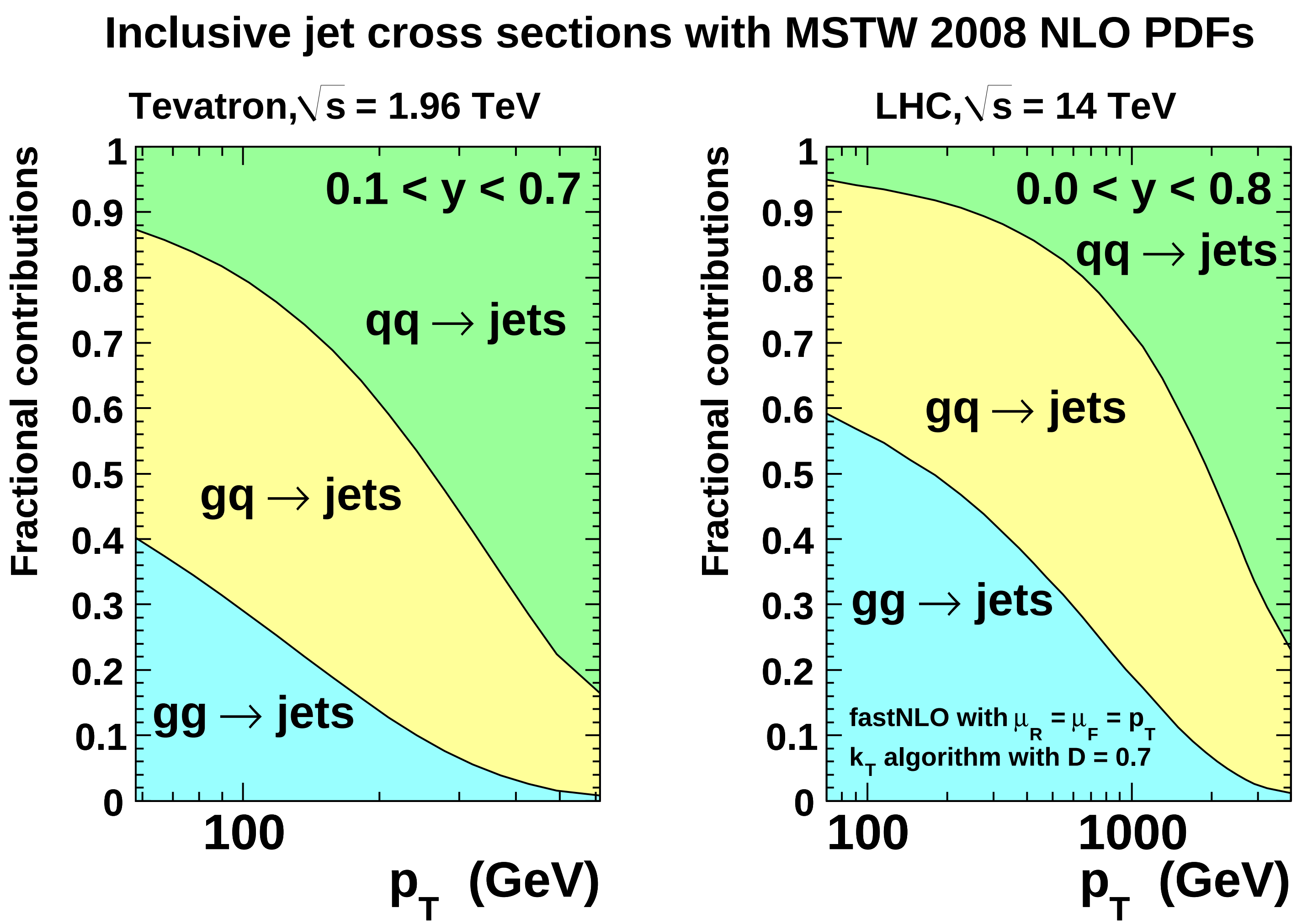

Fraction of jet cross-section made up of different contributions as a function of E_T.

Fit using full treatment of errors perfectly acceptable and determines gluon at $x \sim 0.4$ to about 20% - $xg(x) \sim (1-x)^4$. (Compatible with prompt photon indications.)

Comparison of theory to data for the most recent D0 jet data. Systematic errors shown as band.

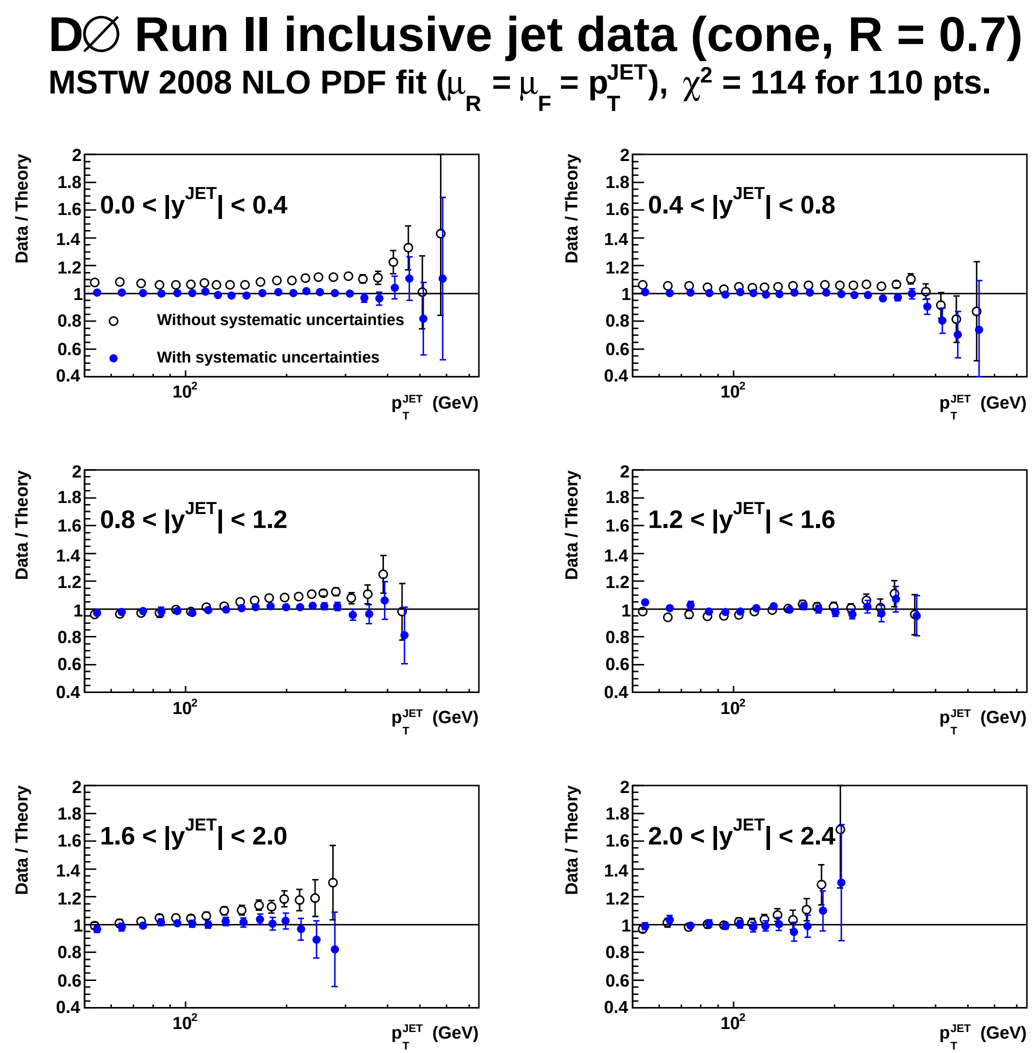

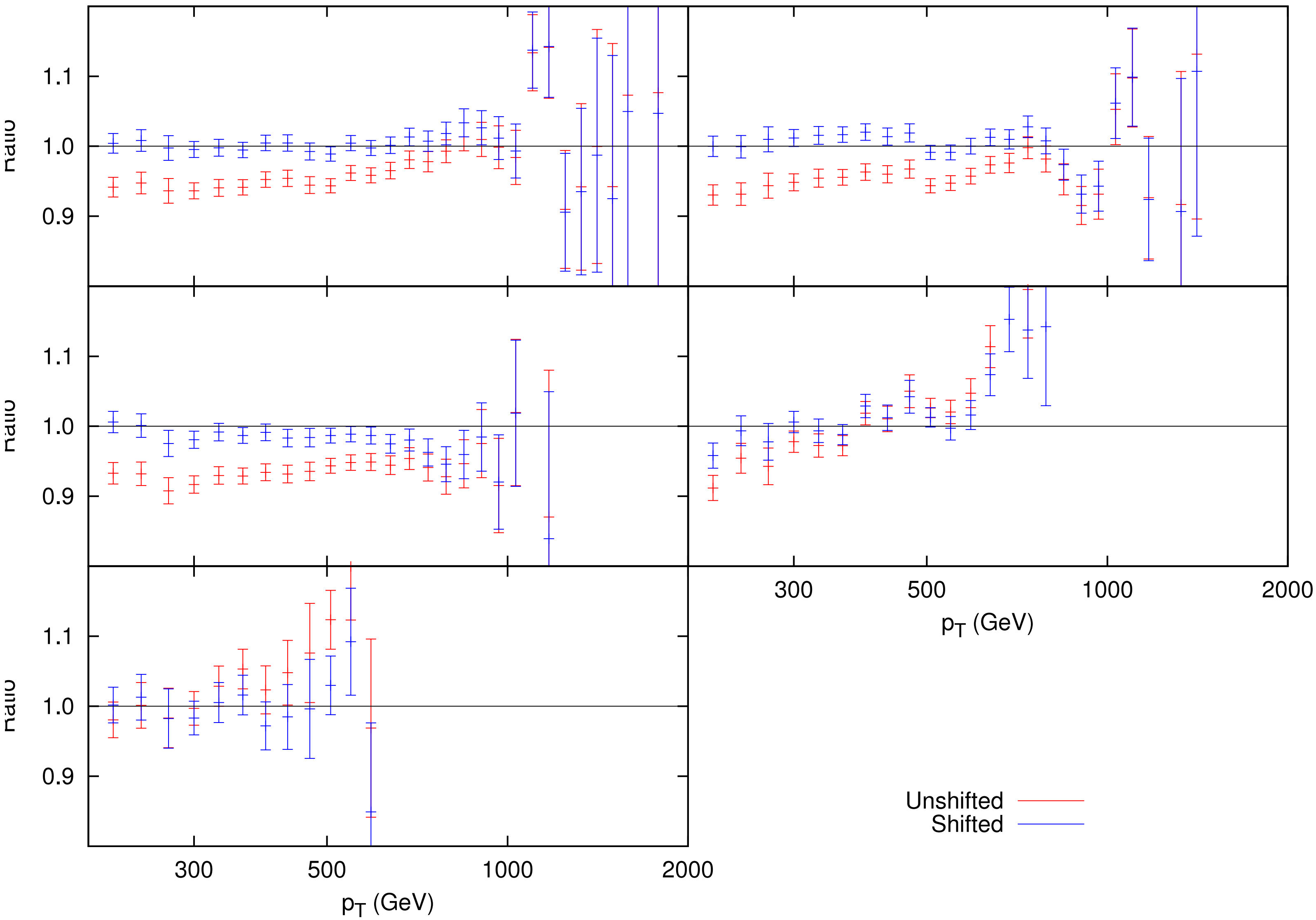

Comparison of theory to data for the most recent CMS jet data.

Small x.

All the above data constrain the partons for $x > 0.05$ (though NMC data extend from higher x down to $x \sim 0.01$). The extension to the region of very low x has been made in the past decade by HERA. Interesting within QCD. Vital for the LHC.

Also important for ultra-high energy cosmic neutrinos.

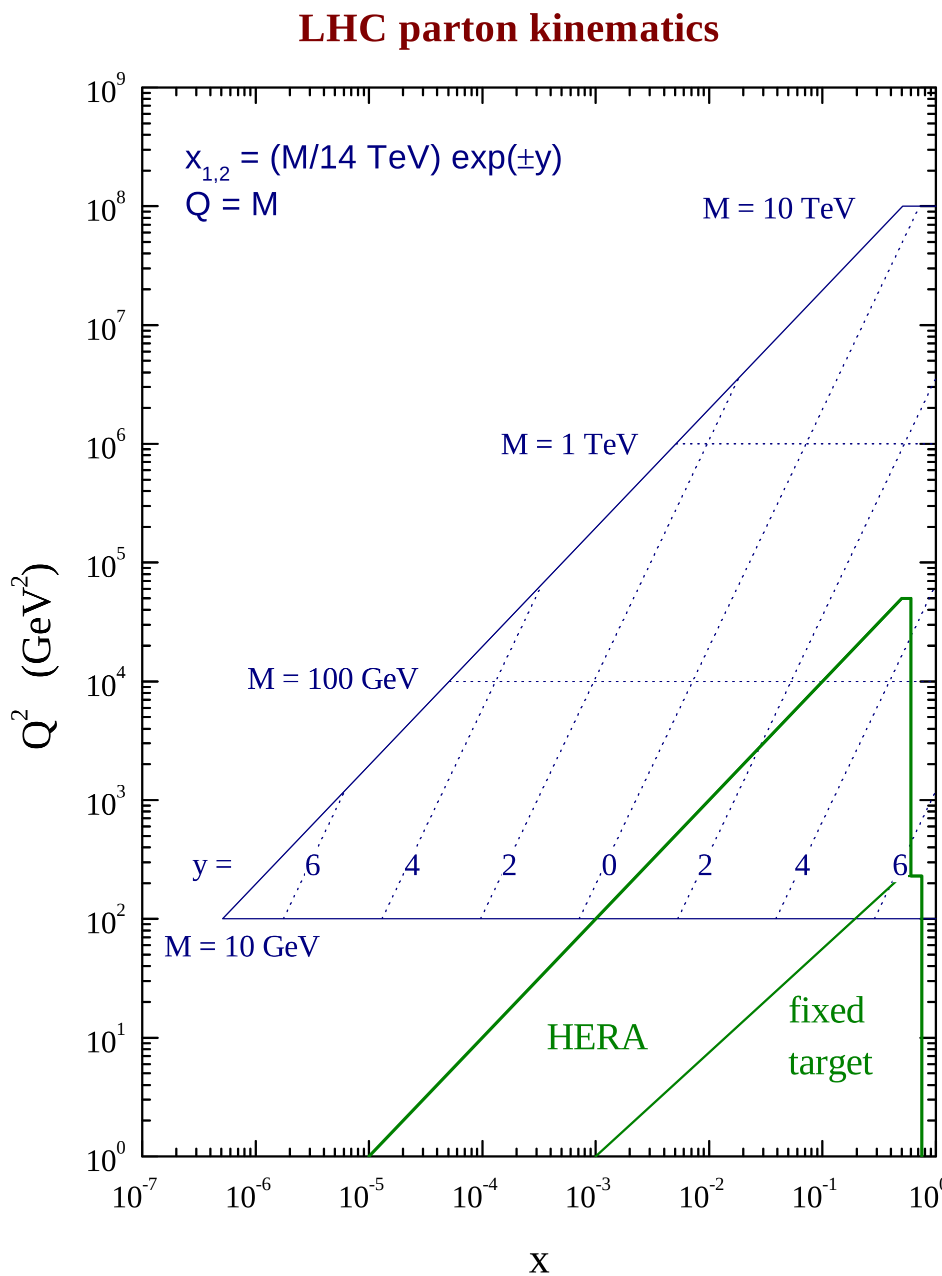

In this region there is very great scaling violation of the partons from the evolution equations and also a great interplay between the quarks and gluons.

Evolution equations for singlet sector are coupled

$$\begin{aligned} \frac{d\tilde{\Sigma}}{d\ln Q^2} &= P_{qq} \otimes \tilde{\Sigma} + P_{qg} \otimes \tilde{g} \\ \frac{d\tilde{g}}{d\ln Q^2} &= P_{gq} \otimes \tilde{\Sigma} + P_{gg} \otimes \tilde{g} \end{aligned}$$

At very small x the splitting functions tend to

$$P^0_{gg} \rightarrow \frac{3\alpha_S}{\pi}\frac{1}{x} \qquad P^0_{qg} \rightarrow 2N_F\frac{\alpha_S}{6\pi}\delta(1-x),$$

and so the gluon grows very quickly with increasing Q^2 while the quark distribution also grows quickly driven by the gluon. Correlation between gluon and $dF_2(x,Q^2)/d\ln Q^2$.

At NLO the small x splitting functions become

$$P^1_{gg} \to -0.7\alpha_S^2 \frac{1}{x} \qquad P^1_{qg} \to 2N_F \frac{\alpha_S^2}{6\pi}\frac{1.6}{x}.$$

Hence, the gluon evolution is only slightly modified, whereas the quark evolution is greatly enhanced at NLO. $dF_2(x,Q^2)/d\ln Q^2$ not directly $\propto xg(x,Q^2)$.

At NNLO the small x splitting functions become

$$P^1_{gg} \to -1.7\alpha_S^3 \frac{\ln(1/x)}{x} \qquad P^1_{qg} \to 2N_F \frac{\alpha_S^3}{6\pi}\frac{1.4\ln(1/x)}{x}.$$

So at NNLO the quark evolution is enhanced yet again while the gluon evolution is suppressed.

It is known that at each subsequent order in α_S each splitting function and coefficient function obtains an extra power of $\ln(1/x)$ (some accidental zeros in P_{gg}), i.e.

$$P_{ij}(x, \alpha_s(Q^2)), \quad C_i^P(x, \alpha_s(Q^2)) \sim \alpha_s^m(Q^2) \ln^{m-1}(1/x).$$

and hence the convergence at small x is questionable.

The global fits usually assume that this turns out to be unimportant in practice, and proceed regardless. The fit is quite good, but could be improved.

Predictions for gluon dominated quantities, e.g. $F_L(x, Q^2)$ (not measured directly at small x very unstable from order to order.

Small x predictions somewhat uncertain.

Comparison of MRST(2008) at LO, NLO and NNLO

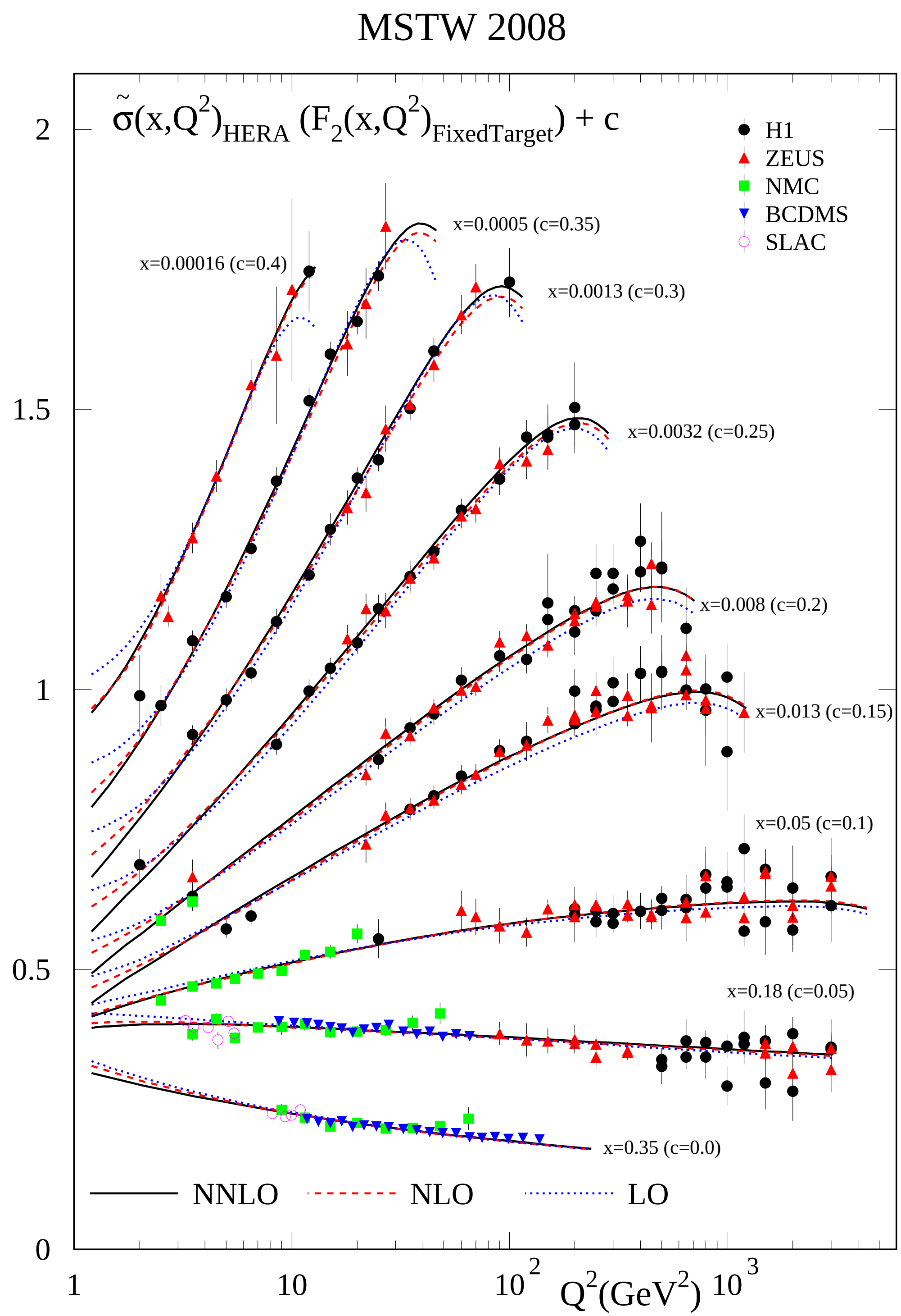

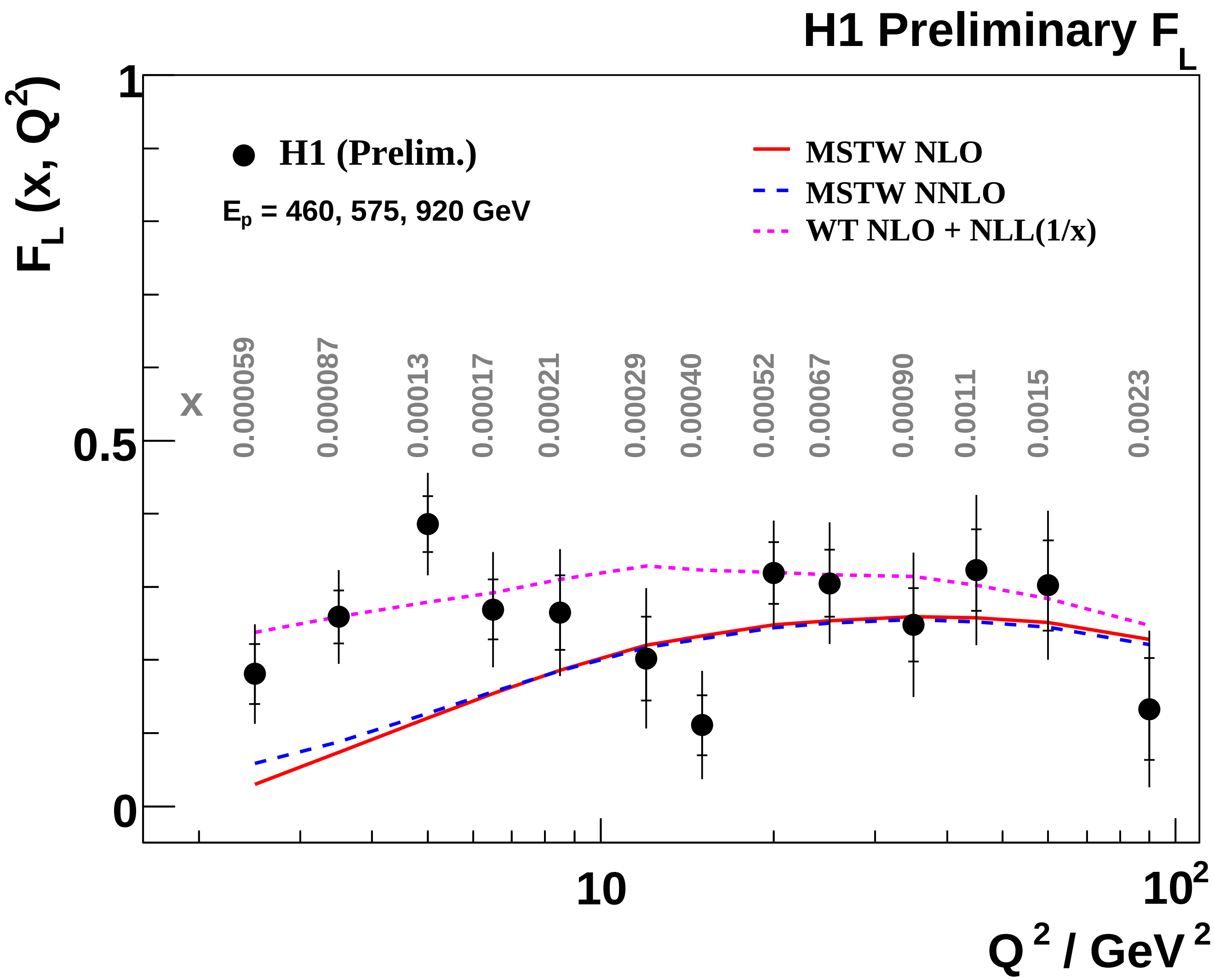

Comparison to H1 prelim data on $F_L(x,Q^2)$ at low Q^2, suggests resummations may be important.

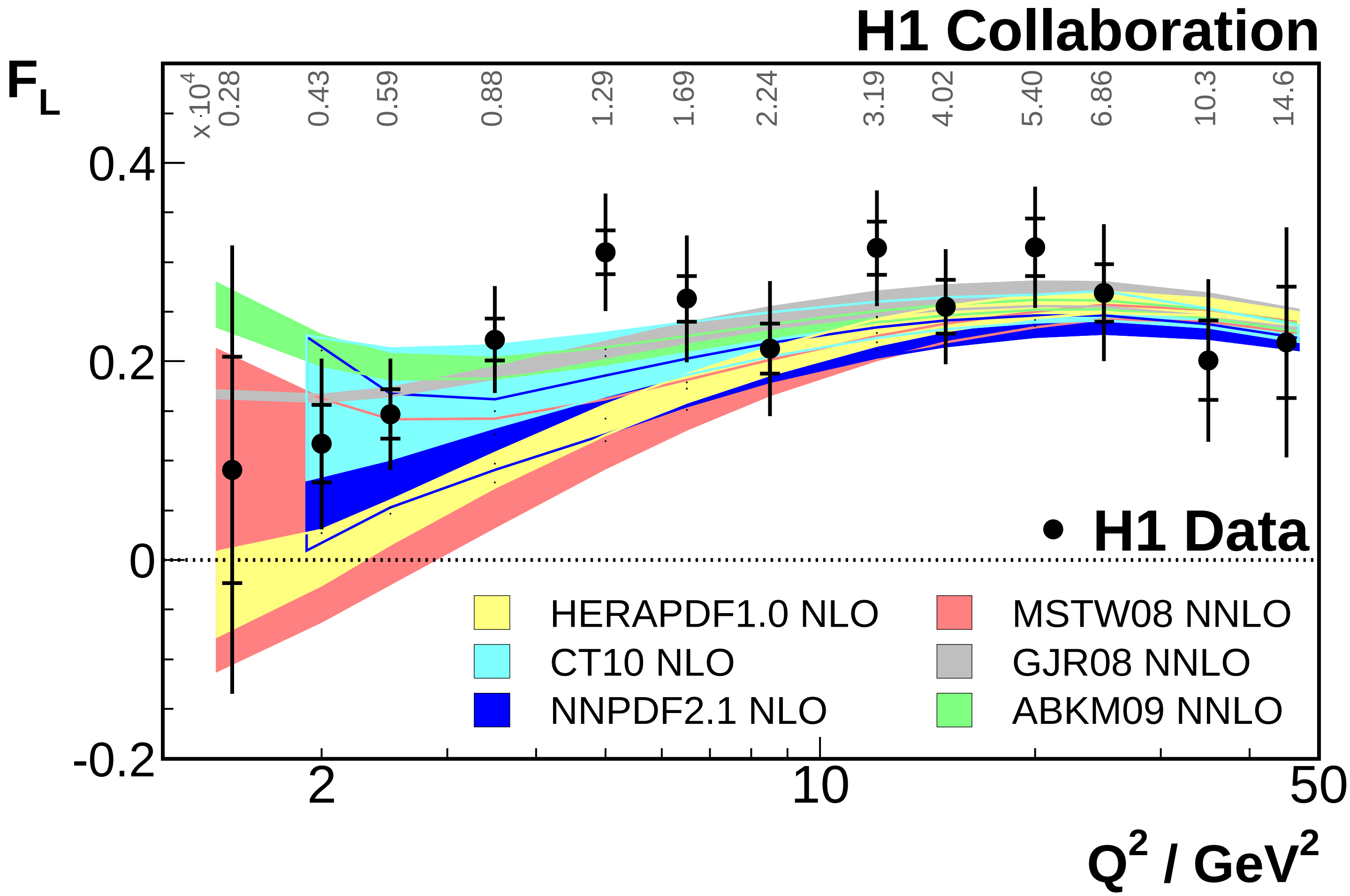

However, quite a large PDF uncertainty (in general) and even larger spread, at fixed order (though differences in definition of order).

Heavy Quarks.

Mainly charm, small contribution from bottom. These are most important at small x. Not only necessary to have correct treatment because of direct data on charm from H1 and ZEUS, but also because charm forms a large component of total structure function at small x.

Two distinct regimes-

Near threshold $Q^2 \sim M_H^2$ massive quarks not partons. Created in final state.

High scales $Q^2 \gg M_H^2$ massless partons. Behave like up, down, strange.

Many analyses still use one or the other. However, more correct to use the theoretically correct description over whole range of Q^2. Known as variable flavour number scheme (**VFNS**) $\rightarrow$ precise definition of parton distributions and scattering at all scales.

Extrapolation between the two simple kinematic regimes for xF_3 measured using neutrino scattering at NuTeV.

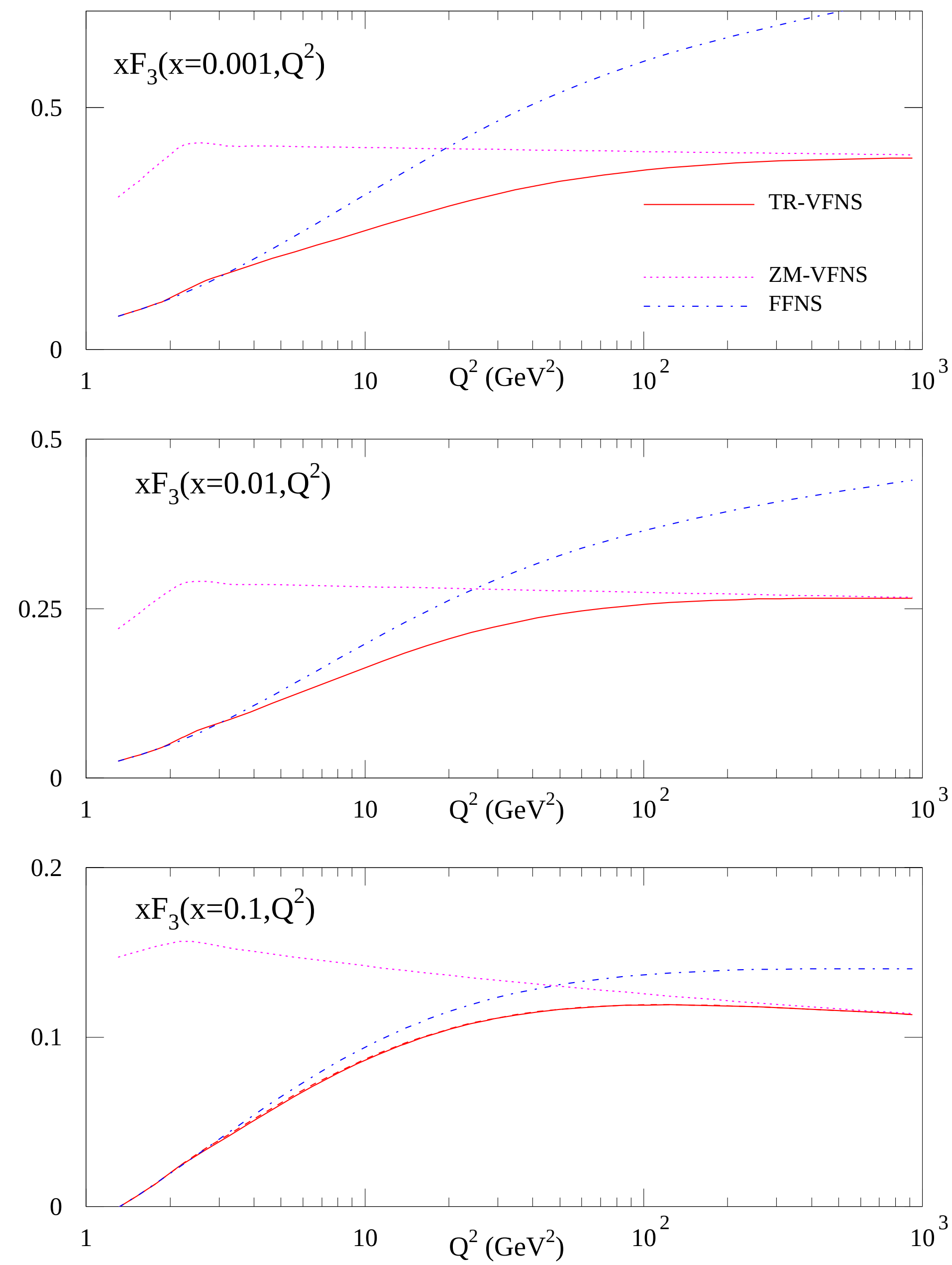

Good description of small x bottom (and charm) data.

Comparison of charm structure function with VFNS theoretical prediction at different orders, and some competitors.

Final data may start differentiating approaches.

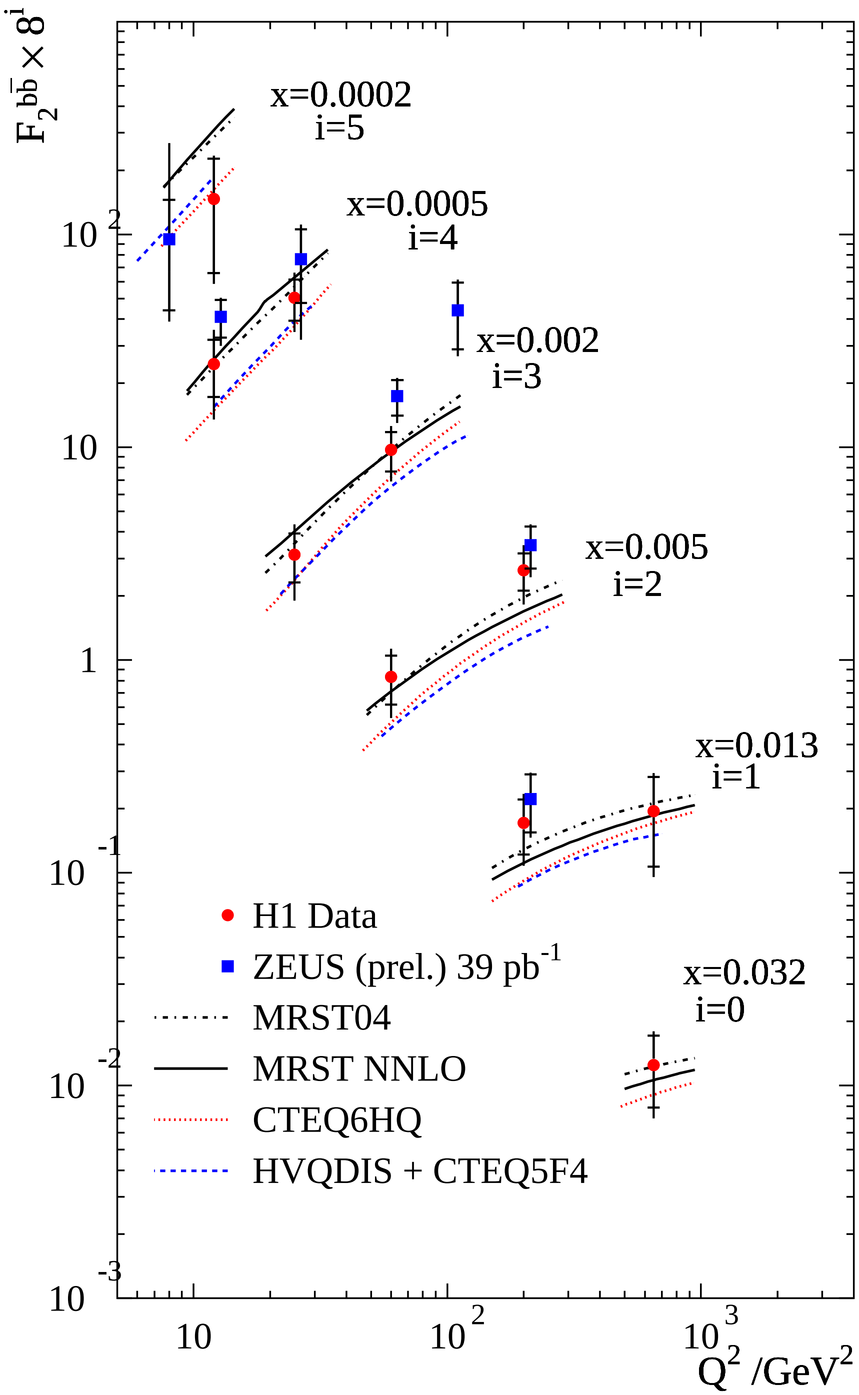

Results.

Above procedure completely determines parton distributions at present. Also determines $\alpha_S(M_Z^2) = 0.120 \pm 0.003\,(\mathrm{expt})$ – as good as most other determinations. Partons and their uncertainties essential input to all LHC and Tevatron studies.